

Electrophysiological and Histopathological Characteristics of Progressive Atrioventricular Block Accompanied by Familial Dilated Cardiomyopathy Caused by a Novel Mutation of Lamin A/C Gene

JUN OTOMO, M.D., SHIGEO KURE, M.D.,* TOMOKO SHIBA, M.D., AKIHIKO KARIBE, M.D., TSUYOSHI SHINOZAKI, M.D., TETSUO YAGI, M.D.,† HIROSHI NAGANUMA, M.D.,‡ FUMIAKI TEZUKA, M.D.,§ MASAETSU MIURA, M.D.,¶ MEIICHI ITO, M.D.,|| JUN WATANABE, M.D., YOICHI MATSUBARA, M.D.,* and KUNIO SHIRATO, M.D.

From the Departments of Cardiovascular Medicine and *Medical Genetics, Tohoku University Graduate School of Medicine, Sendai; †Department of Cardiovascular Medicine and ‡Pathology, Sendai City Hospital, Sendai; §Department of Pathology, National Sendai Hospital, Sendai; ¶Department of Cardiovascular Medicine, Furukawa City Hospital, Furukawa; and ||Ito Clinic, Kami, Japan

Conduction Defect Caused by Lamin A/C Gene Mutation. *Introduction:* Mutations of lamin A/C gene (*LMNA*) cause dilated cardiomyopathy (DCM) with atrioventricular (AV) conduction defect, although the electrophysiological and histological profiles are not fully understood.

Methods and Results: We analyzed a large Japanese family (21 affected and 203 unaffected members) of DCM with AV block. The responsible *LMNA* mutation of IVS3-10A>G was novel and caused an aberrant splicing. The first clinical manifestation was low-grade AV block or atrial fibrillation (AF), which developed in affected members aged ≥ 30 years. We observed that the AV block progressed to third-degree within several years. The electrophysiological study of the four affected members revealed an impairment of intra-AV nodal conduction. Because of advanced AV block, pacemakers were implanted in 14 out of 21 affected members at the mean age of 44 years. Three affected members died suddenly and two affected members died of heart failure and/or ventricular tachycardia (VT) even after the pacemaker implantation. Postmortem examination showed conspicuous fibrofatty degeneration of the AV node. Endomyocardial biopsies showed remarkably deformed nuclei and substantial glycogen deposits in the subsarcolemma.

Conclusion: The clinical phenotype in this family was characterized by (1) the first manifestation of the prolonged PQ interval or AF in adolescence, (2) progressive intra-AV nodal block to the third degree in several years, and (3) progressive heart failure after pacemaker implantation. Histological study revealed preferential degeneration at the AV node area and novel cellular damages in the working myocardium. (*J Cardiovasc Electrophysiol*, Vol. 16, pp. 137-145, February 2005)

lamin A/C, dilated cardiomyopathy, atrioventricular block, atrial fibrillation, gene

Introduction

Two polypeptides, lamin A and lamin C, are encoded by the lamin A/C gene (*LMNA*). These arise through alternative splicing of the same primary transcript.^{1,2} Lamin A and lamin C proteins are components of the nuclear envelope, forming the inner and the outer nuclear membranes, the nuclear pore complex, and the nuclear lamina.³ It has been reported that mutations in the *LMNA* cause various genetic diseases referred to as "laminopathy."⁴ To date, seven different types of laminopathies have been established: autosomal dominant⁵/recessive⁶ Emery-Dreifuss muscular dys-

trophy, limb-girdle muscular dystrophy 1B,⁷ familial partial lipodystrophy,⁸ sensory and motor axonal neuropathy Charcot-Marie-Tooth disorder type 2,⁹ mandibuloacral dysplasia,¹⁰ Hutchinson-Gilford progeria syndrome,¹¹ and autosomal dominant dilated cardiomyopathy (DCM) with conduction defect.¹²

The laminopathies have two major cardiac phenotypes, progressive atrioventricular (AV) block, and myocardial damage. The AV block in the laminopathies is mostly accompanied by cardiomyopathy, but isolated AV block was reported in limb girdle muscular dystrophy 1B^{7,13} and autosomal dominant DCM with conduction defect.¹⁴ We found a large family with DCM with progressive AV block caused by a novel mutation of *LMNA* and provide the clinical, genetic, electrophysiological, and histopathological findings concerning this particular familial DCM.

Methods

Participation of the Family

This familial DCM was first identified by the high incidence of pacemaker implantation (PMI). We started the investigation of the family because the preliminary study revealed a

This study was supported by a grant from the Ministry of Education, Culture, Sports, Science, and Technology, and a grant from the Ministry of Health, Labor, and Public Welfare.

Address for correspondence: Jun Watanabe, M.D., Department of Cardiovascular Medicine, Tohoku University Graduate School of Medicine, 1-1, Seiryomachi, Aoba-ku, Sendai, 980-8574, Japan. Fax: +81-22-717-7156; E-mail: watanabe@cardio.med.tohoku.ac.jp

Manuscript received 1 March 2004; Revised manuscript received 11 September 2004; Accepted for publication 20 September 2004.

doi: 10.1046/j.1540-8167.2004.40096.x

high incidence of not only PMI but also DCM (Fig. 1A). Written informed consent was obtained from all participants under approval of the local ethics committee. The family members showing DCM on echocardiogram were designated as affected irrespective of the presence of the conduction defect. The members who died suddenly or died of heart failure without otherwise known causes were also regarded as affected. We collected clinical data of the affected members from the medical records, which included 12-lead electrocardiogram (ECG), transthoracic echocardiogram, and serum creatine kinase. The data of cardiac catheterization and postmortem examination were also evaluated when available. Neurological assessment was performed for clinically affected members by review of medical records, blood examination of serum creatine kinase, and clinical neuromuscular examination evaluated by neurological experts. The family members (≥ 30 years of age) showing no cardiac phenotypes were designated as unaffected. We examined ECG, echocardiogram, and serum creatine kinase in some unaffected members.

Mutational Analysis of LMNA

We obtained 5–10 mL blood samples from each family member. Genomic DNA was extracted from the whole blood in 25 family members or heart tissue obtained at autopsy.

Because the *LMNA*-mutated DCM with conduction defect was known, we first screened for mutations of *LMNA*.¹² Twelve coding exons of *LMNA* were amplified by polymerase chain reaction (PCR) in the proband (IV-70 in Fig. 1A) as described.¹² Direct sequencing analysis was performed with an automated fluorescence sequencer (ABI PRISM 310, PE-Biosystems, Foster City, CA) by the dye-primer cycle sequencing method as described.¹⁵ The PCR-based restriction fragment length polymorphism (PCR-RFLP) analysis was performed in family members and in 100 chromosomes from 50 normal volunteers (randomly selected from our control genomic store, ≥ 30 years of age) to test whether the mutation was a polymorphism by using a modified forward primer, 5'-CCAGCACTCAGCTCCCAGGT-3' and a reverse primer, 3'-TGGTCTCACGCAGCTCCTGGAAGCG-5'. The underlined nucleotide represents an introduced mismatch, which generated a recognition site for *HhaI* in DNA fragments amplified from the mutant allele. The thermoprofile consisted of initial denaturing of 95°C for 3 min, 35 cycles of 98°C or 10 seconds, 55°C for 30 seconds, and 72°C for 30 seconds, followed by 72°C for 7 min. A total of 10 μ L of PCR products were digested with 10 units of *HhaI* at 37°C overnight followed by 4% agarose gel electrophoresis. The DNA fragments were stained with ethidium bromide and visualized on a UV transilluminator.

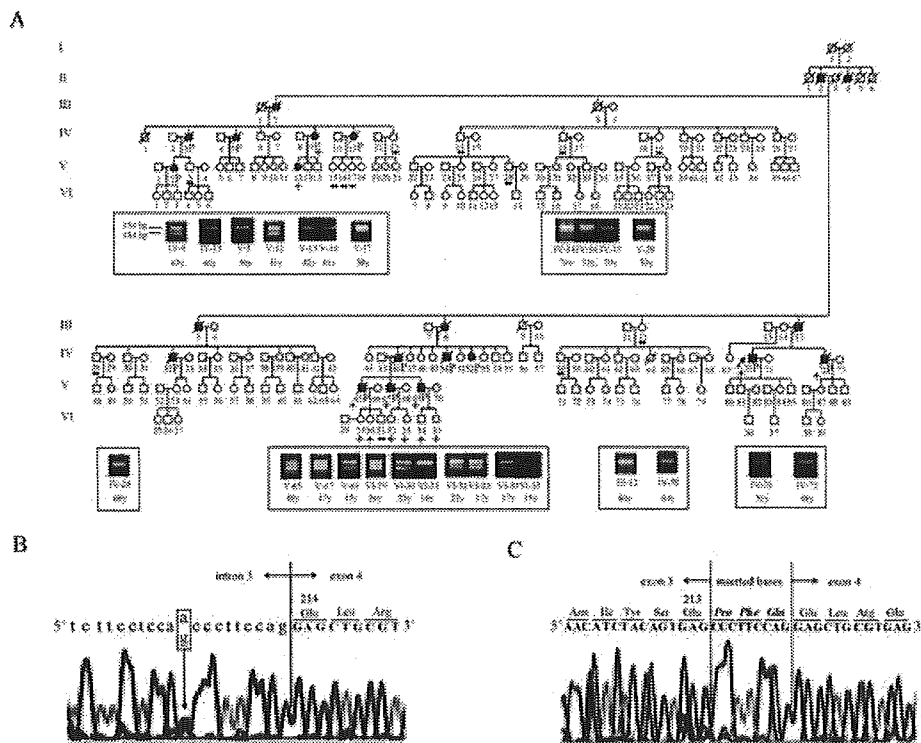


Figure 1. The family pedigree and *LMNA* mutation. (A) The family pedigree with DCM with conduction defect caused by the *LMNA* mutation. Circles and squares indicate male and female, respectively. Closed circles and squares indicate affected members. Roman and arabic numerals indicate generation and case numbers. The letter P indicates affected members who received pacemaker implantation. Slash means deceased. Plus and minus indicate presence and absence of the mutation, IVS3–10A>G, respectively. An arrow indicates the proband. The photographs in boxes show electrophoresis of *HhaI*-digested PCR by PCR-RFLP analysis. Two DNA fragments of 156 bp and 134 bp show the presence of the mutation, IVS3–10A>G, while only the fragment of 156 bp shows the absence of the mutation. (B) Direct sequencing analysis of the *LMNA* mutation. The proband had a heterozygous base substitution from adenine (a) to guanine (g) at 10-base upstream from the junction between intron 3 and exon 4 (IVS3–10A>G, arrow points). Numbers above the amino acid symbols indicate the codon number. (C) A cDNA analysis of the *LMNA* mutation. Direct sequencing analysis of a cDNA fragment of 158 bp reveals insertion of nine bases, 5'-CCCTTCCAG-3', in the junction between exon 3 and exon 4. Amino acid symbols in bold and italic represent three codons inserted into the exon 3/exon 4 junction.

Analysis of LMNA mRNA of a Lymphoblast Cell Line Established from a Patient

A lymphoblast cell line was established from a blood sample of the proband by Epstein-Barr virus infection. Total RNA was purified from the lymphoblasts with RNeasy Mini kit (Qiagen, Germany) and subjected to reverse transcription as described.¹⁵ A cDNA fragment containing the exon 3/exon 4 junction was amplified by PCR with a forward primer, 5'-GAGAACAGGCTGCAGACCAT-3', and a reverse primer, 3'-TTGTCAATCTCCACCAGTC G-5'. The RT-PCR products were size-separated by 5% NuSieve GTG agarose (FMC BioProducts, Rockland) gel electrophoresis, and cDNA fragments of 149 bp and 158 bp in size were excised for direct sequencing analysis as described above.

Electrophysiological and Histological Examination

Conventional electrophysiological (EP) study was performed in four affected members because of AV block. Three standard electrode catheters were positioned in the high right atrium, His bundle region, and RV. A quadripolar-catheter or octapolar-catheter was inserted into the coronary sinus and positioned to record the coronary sinus electrogram using each pair of electrodes. The EP study included standard diagnostic protocols for sinus nodal function, AV nodal function,

and ventricular tachycardia (VT) induction.¹⁶ Briefly, in the induction of VT, up to three extrastimuli were induced (coupling intervals \geq 180 ms) from the apex and the outflow tract of the RV after conditioning pacing (basic cycle length = 600 or 400 ms). If negative, we repeated the protocol above under intravenous administration of isoproterenol (started at 0.5 μ g/min, a target heart rate was 20% increase from the control).¹⁷

Histopathological examination was performed in two postmortem heart samples obtained from affected members (IV-72, V-65) and in four biopsied samples of endomyocardial tissues taken from the septum and apex of the RV. Light and electron microscopical analysis was performed.

Results

Clinical Characteristics of Affected Family Members

The clinical characteristics of 21 affected members are summarized in Table 1. Information concerning the first manifestation was available in six affected members: first- or second-degree AV block and/or atrial fibrillation (AF) initially developed in five of the six affected members, IV-70, V-12, V-65, V-67, and V-69, while affected member IV-72 presented congestive heart failure with AF and third-degree

TABLE 1
Clinical Characteristics of Clinically Affected Members in the Family with Lamin A/C Gene Mutation

Case No.	Gender	Clinical Course			Echocardiogram					Comment
		Onset (age)	PMI (age)	Cause of Death (age)	Age	LVEDD/ESD (mm)	LVEF (%)	LAD (mm)	MD	
II-2*	M	ND	No	53 y CHF					ND	
II-4*	F	ND	No	51 y SD					ND	
III-2*	F	ND	No	58 y CHF					ND	
III-5*	M	ND	No	55 y CHF					ND	
III-8*	F	ND	No	45 y SD					ND	
III-15*	M	ND	No	59 y CHF					ND	
IV-3*	F	ND	50 y	71 y cause unknown					ND	
IV-5*	F	ND	50 y	59 y apoplexy					ND	
IV-9	F	ND	49 y	64 y live					ND	
IV-11*	F	ND	40 y	58 y CHF and VT					ND	
IV-32*	M	ND	37 y	55 y SD					ND	
IV-46*	F	ND	45 y	62 y SD					ND	
IV-50*	M	ND	Yes	Age and cause unknown					ND	
IV-52*	F	ND	Yes	Live; age unknown					ND	
IV-70	M	42 y first- to second-degree AVB and AF (QRS = 0.10 sec)	45 y high-degree AVB and AF	53 y live	42 y	55/38	68	35	NM	43 y Holter ECG; four consecutive PVCs CK 79 (mU/mL) (<197 mU/mL)
					45 y	61/42	69	38		
					53 y	61/45	60	47		
IV-72	M	47 y CHF and third-degree AVB with AF (QRS = 0.10 sec)	47 y third-degree AVB with AF	50 y SD	47 y	69/56	36	55	NM	Diabetes mellitus, 48 y spontaneous sustained VT, CK 155 (mU/mL) (<200 mU/mL)
					49 y	66/65	33	55		
					50 y	76/67	24	58		
V-2*	F	ND	38 y	54 y live					ND	DCM
V-12	F	41 y first-degree AVB (PR = 0.22 sec, QRS = 0.08 sec)	No	42 y live	41 y	43/30	65	23	NM	41 y Holter ECG; couplet PVCs, Ergometer; PVC increased
V-65	M	42 y paroxysmal AF (QRS = 0.10 sec)	45 y high-degree AVB and AF	48 y CHF and VT	45 y	59/44	51	42	NM	47 y spontaneous sustained VT (LBBB+inferior axis type) CK 134 (mU/mL) (<195 mU/mL)
					48 y	60/53	23	43		
V-67	M	37 y paroxysmal AF (QRS = 0.10 sec)	43 y high-degree AVB and AF	49 y live	43 y	56/47	31	43	NM	47 y spontaneous sustained VT (RBBB+superior axis type) CK 134 (mU/mL) (<195 mU/mL)
					47 y	62/43	58	49		
V-69	M	30 y first- to second-degree AVB (QRS = 0.11 sec)	37 y third-degree AVB	47 y live	39 y	52/45	31	43	NM	38 y spontaneous sustained VT (RBBB+inferior axis type) 42 y performed catheter ablation for VT, CK 49 (mU/mL) (<195 mU/mL)
					44 y	60/47	41	41		

*Clinically affected member whose DNA was not available for the study. AF = atrial fibrillation; AVB = atrioventricular block; CHF = congestive heart failure; CK = creatine kinase; DCM = dilated cardiomyopathy; F = female; LAD = left atrial diameter; LBBB = left bundle branch block; LVEDD/ESD = left ventricular end-diastolic/end-systolic diameter; LVEF = left ventricular ejection fraction; M = male; MD = skeletal muscle disorder; ND = not detectable; y = year; NM = no manifestation; PMI = permanent pacemaker implantation; PVC = premature ventricular contraction; RBBB = right bundle branch block; SD = sudden death; VT = ventricular tachycardia.

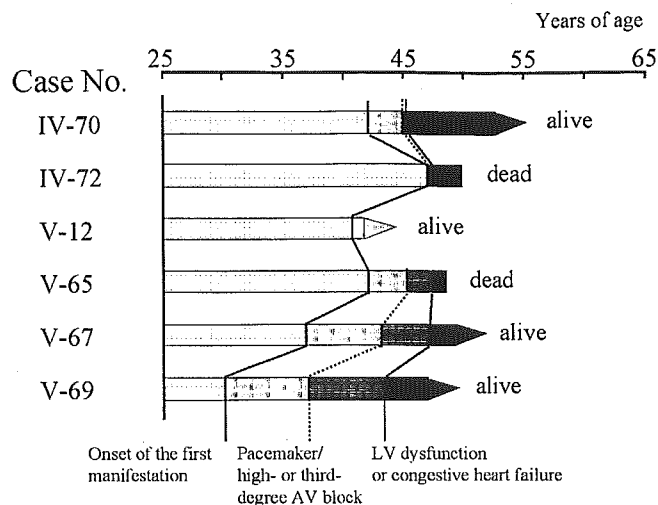


Figure 2. Onset and time course of AV block and LV dysfunction. The onset and the time course of AV block and LV dysfunction are illustrated. The first manifestation, including first- or second-degree AV block and/or AF, occurred at 30 to 47 years of age. In four out of six affected members, AV block progressed to third-degree AV block, and these members received pacemaker implantation within 3 to 7 years. In two dead affected members, the first manifestation was more likely to occur later and progressed rapidly. LV dysfunction was defined by LV diameter ≥ 60 mm or LV ejection fraction $\leq 40\%$.

AV block at the onset of the disease (Fig. 2). The age of onset ranged from 30 to 47 years with a mean age of 40 years. At the first manifestations, all affected members had normal width of QRS complex, and intraventricular conduction delay was not found. Because of the progression to advanced AV block, 14 of the 21 affected members received pacemakers, and six affected members died before pacemakers were clinically available. One affected member, V-12, was 42 years old and had only first-degree AV block. The mean age of PMI was 44 years with a range of 37–50 years. The PMI was needed within 7 years from the first manifestations such as first- or second-degree AV block and/or AF (Fig. 2). The width of QRS complex remained normal at the PMI. Fourteen of the 21 affected members have died, and the affected members with pacemakers died at a mean age of 57 (48–71) years, while the affected members without pacemakers died at a mean age of 53 (45–59) years. Sudden death was observed in five of these 14 affected members and six affected members died of congestive heart failure or fatal VT. The affected members, IV-70, V-12, V-65, V-67, and V-69, showed no clinical symptoms of congestive heart failure at the first manifestation. In affected members, IV-70 and V-12, echocardiography revealed normal LV dimensions and cardiac function. After the first manifestation, affected member IV-70 showed the progression of LV dilatation within 3 years. Echocardiographical LV dysfunction (LV diameter ≥ 60 mm, or LV ejection fraction $\leq 40\%$) was found 6 years after the first manifestation in affected member V-65, 6 years later in affected member V-67, and 9 years later in affected member V-69. The affected member, IV-72, first visited a hospital for clinical heart failure with third-degree AV block. No documentation was available concerning whether heart failure was followed by AV block (Fig. 2). In the general neurological assessment, no skeletal muscle abnormalities were found by neurological experts or in the review of medical records of clinically affected members in the family. Four genetically affected members (IV-70, IV-72, V-65, and V-69) were extensively evaluated by neurological experts and no manifestation such as Emery-Dreifuss muscular dystrophy, limb-girdle muscular dystrophy, or Charcot-Marie-Tooth disorder was found.

Serum creatine kinase was within the normal range in some affected members (IV-70, IV-72, V-65, and V-69).

Identification of LMNA Mutation

All coding regions of *LMNA* were screened for mutations in a DNA sample of the proband (IV-70). Direct sequencing analysis did not reveal any base change in each exon, but a heterozygous base substitution from adenine to guanine was detected 10-base upstream of the intron 3/exon 4 junction (IVS3–10A>G) (Fig. 1B). We screened for the IVS3–10A>G by direct sequencing and PCR-RFLP analysis in 19 members (≥ 30 years of age), which included seven affected (IV-9, IV-70, IV-72, V-12, V-65, V-67, V-69) and 12 unaffected members (III-12, IV-13, IV-14, IV-16, IV-19, IV-28, IV-58, V-3, V-15, V-16, V-17, V-28), and in seven members (< 30 years of age) showing no cardiac phenotype (VI-29, VI-30, VI-31, VI-32, VI-33, VI-34, VI-35) whose fathers are affected members. The IVS3–10A>G mutation was detected in all the seven members, but not in all the 12 unaffected members. Furthermore, the mutation was detected in six of the seven members (< 30 years of age) showing no cardiac phenotype. Results of the PCR-RFLP analysis are shown in Figure 1A. On the other hand, the mutation was not detected in 100 control alleles (data not shown). These results suggested that the mutation was tightly associated with the disease and that there were mutant carriers (< 30 years of age) before the onset of the disease.

The RT-PCR study revealed two cDNA fragments of 149 and 158 bp in size in the proband (data was not shown), while only the 149-bp fragment was observed in the control (data was not shown). Direct sequencing analysis showed that a nine-base fragment, 5'-CCCTTCCAG-3', was inserted in the junction between exon 3 and exon 4 in the 158-bp fragments (Fig. 1C). These results suggested that the IVS3–10A > G altered a splicing site to the 10th nucleotide (a/g heterozygous) upstream from the 3' end of the intron 3 from the junction between the intron 3 and exon 4 (Fig. 1B).

TABLE 2
Electrophysiological Characteristics of Affected Members with Lamin A/C Gene Mutation

Case No.	Gender	Age	Electrophysiological Conductive Parameters							Induced Arrhythmia		
			P Duration (ms)	PR Interval (ms)	PA Interval (ms)	AH Interval (ms)	HV Interval (ms)	QRSS Duration (ms)	Wenckebach Rate at Atrial Pacing (beats/min)	Atrial Arrhythmia	Ventricular Arrhythmia	
IV-70	M	45	110	470	30	370	55	100	100	AF (before EPS)	NP	
V-65	M	45	120	565	30	460	55	100	50	AF (before EPS)	Sustained VT (LBBB+inferior axis type)	
V-67*	M	43	AF	AF	AF	AF	50	100	AF	AF	NI	
V-69	M	42	140	Wenckebach	80	Wenckebach	40	110	During sinus rhythm	NP	Sustained VT (RBBB+inferior axis type)	

* During sinus rhythm before EPS, administration of 1.0 mg of atropine sulphate improved Wenckebach-type AV block to one to one AV conduction. AF = atrial fibrillation; EPS = electrophysiological study; LBBB = left bundle branch block; M = male; NI = not induced; NP = not performed; RBBB = right bundle branch block; VT = ventricular tachycardia.

Electrophysiological and Histopathological Characteristics

EP study was performed in four affected members, IV-70, V-65, V-67, and V-69, because of bradycardia and/or spontaneous VT (Table 2). The EP study indicated that affected members, IV-70 and V-65, had AV nodal dysfunction with marked prolongation of the AH interval. In contrast, the HV interval and QRS duration were normal in all four affected members, indicating that the conduction systems of the infra-

His bundle to Purkinje fiber and intraventricles might not be impaired. Although affected member, V-65, had AF (Fig. 3A), the AV conductivity was evaluated after DC defibrillation. He demonstrated Wenckebach-type second-degree AV block (Fig. 3B) with prolonged AH interval (Fig. 3C). Furthermore, VT could be reproducibly induced by programmed stimulation to the outflow tract of the RV (Fig. 3D).

Heart specimens were obtained at autopsy from affected members, IV-65 and V-72. Microscopical examination disclosed marked fibrofatty degeneration in the AV junction and

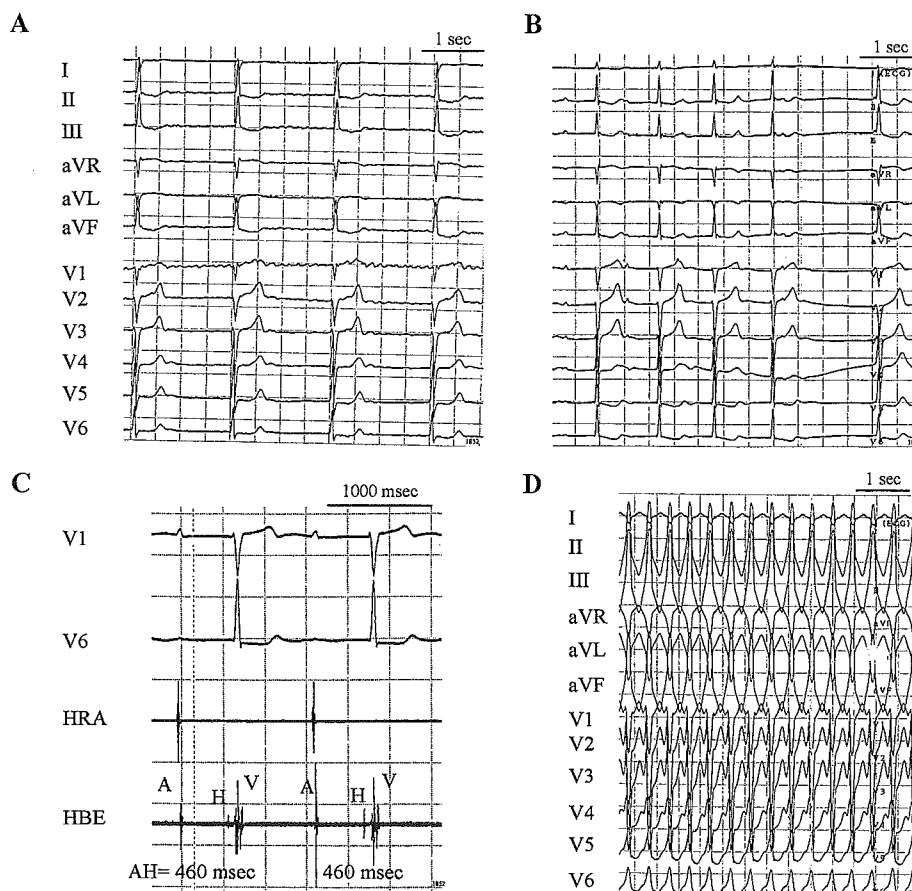


Figure 3. Twelve-lead ECGs and intracardiac electrogram. Cardiograms were recorded during the electrophysiological study of affected member, V-65. At the beginning of the electrophysiological study, (A) AF with complicated third-degree AV block (30 ventricular beats/min) was found. (B) After a direct current defibrillation, the sinus rhythm appeared in association with Wenckebach-type second-degree AV block. (C) In the intracardiac electrogram a prolonged AH interval (460 ms) was detected during the sinus rhythm. (D) Sustained VT could be induced by programmed stimulations at the out-flow tract of the RV. HRA and HBE indicate high right atrium and His bundle electrogram, respectively.

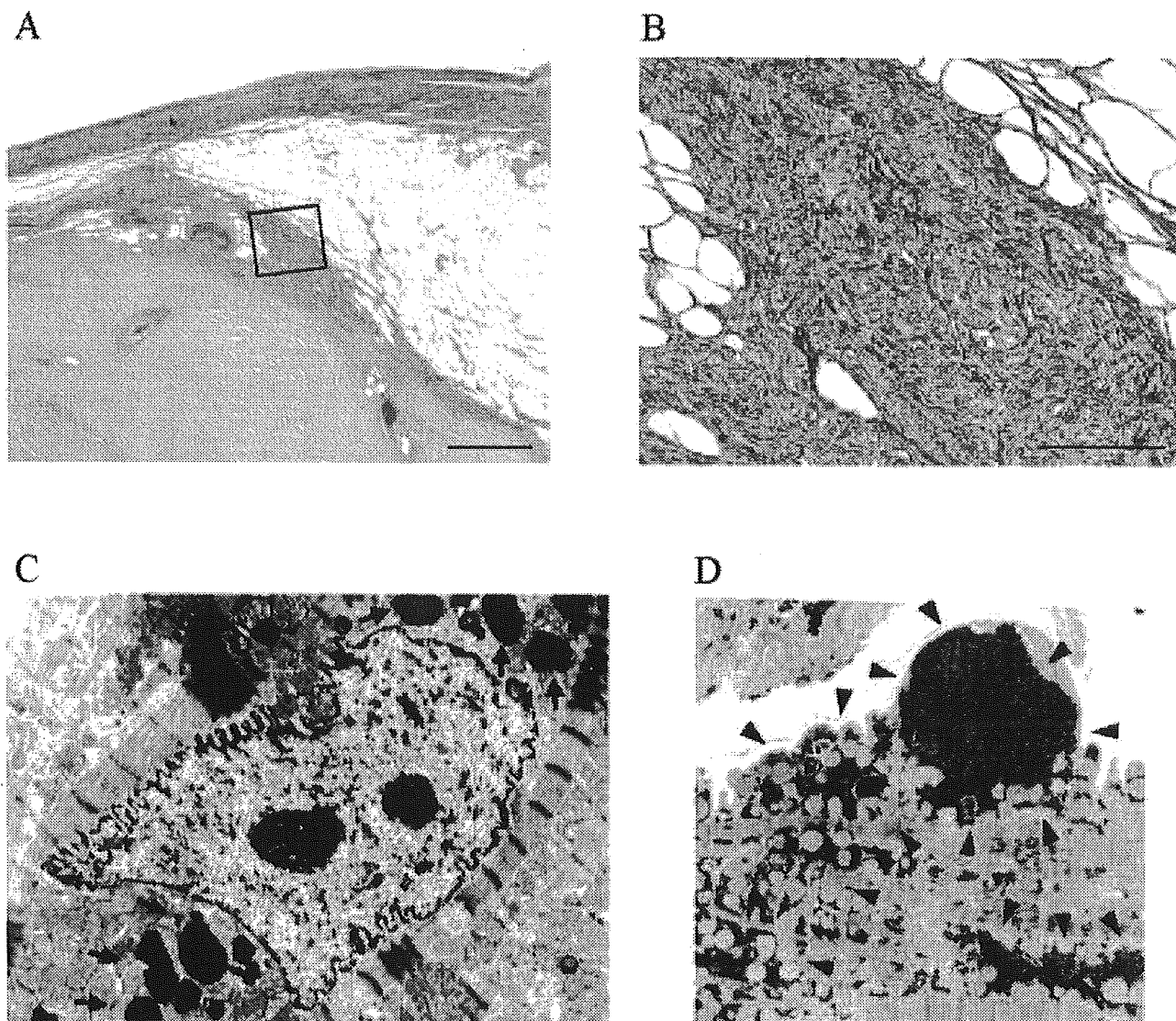


Figure 4. Light and electron microgram. Light microscopic examination of the AV junction in affected member V-65 by Elastica-Masson staining revealed atrophy of the AV node with fibrofatty degeneration (Panel A). The boxed area in (Panel A) is shown with a higher magnification in (Panel B). The number of pacemaker cells appears to be decreased in the AV node in (Panel B). Electron microscopic analyses of myocardium samples obtained from affected member V-65 by biopsy showed deformed nuclei with increased lipofuscin (Panel C, arrows) and accumulated glycogen granules around the mitochondria and beneath the subsarcolemma (D, arrow heads). Scale bars in (Panel A) and (Panel B) represent 500 and 100 μm , respectively.

advanced atrophy of the AV node (Fig. 4A), and fibrosclerotic degeneration in the AV node associated with decreased numbers of pacemaker cells (Fig. 4B). Endocardial biopsy of the RV was performed in affected members, IV-46, V-65, V-67, and V-69, and light microscopical examination revealed interstitial fibrosis and contraction band without the disarray arrangement (data are not shown). Electron microscopy demonstrated a large number of deformed nuclei with increased lipofuscin (Fig. 4C) and a prominent accumulation of glycogen deposits beneath the subsarcolemma and around the mitochondria (Fig. 4D). The nuclear membrane integrity was preserved in all of the examined specimens.

Discussion

We examined familial DCM with progressive AV block in a large Japanese family and identified a novel *LMNA* mutation of IVS3-10A>G. Affected members initially showed

problems in ECG such as first- or second-degree AV block and/or AF at 30–40 years of age without detectable LV dysfunction. Progression to third-degree AV block was observed in 14 affected members, and they received pacemakers within several years of the first ECG finding. Unfortunately, seven affected members died suddenly or unexpectedly even after the pacemakers were implanted. Some affected members with PMI died from congestive heart failure. The EP study disclosed that the conduction defect occurred predominantly in the AV nodal area as compared with the ventricular area, which was supported by the histological findings that the fibrofatty degeneration was more striking in the AV node than in the atrial or ventricular wall.

The *LMNA* Mutation in Familial DCM with Conduction Defect

Since introns are noncoding sequences, a mutation in an intron does not usually cause an mRNA abnormality.

However, the present mutation of the intron (IVS3-10A>G) created an aberrant splicing site between intron 3 and exon 4. The missplicing arose at the 10th nucleotide (a/g) upstream of the 5' end from the 3' end of intron 3 (Fig. 1B), and consequently inserted nine bases to the 5' end of exon 4. The genetic approach strongly indicated that this mutation has a close relation to the clinical phenotype. In fact, the mutation was never found in unaffected family members and 50 volunteers. Although we showed the insertion of the nine bases in the cDNA assay with RT PCR, we did not show the insertion at the protein level. Protein analysis would be important, especially for confirming the present interpretation and for future functional analyses of the protein.

Although the relationship between the mutation site of *LMNA* and the clinical phenotypes of the laminopathies remains unclear, this mutation was novel and first described in the present study. It also remains unknown why laminopathies due to the *LMNA* mutations have various clinical phenotypes. Further studies are necessary to elucidate the relationship between the phenotype and the prognosis of laminopathies and the *LMNA* mutations.¹⁸⁻²⁰

The incidence of the *LMNA*-mutated DCM with AV conduction defect remains controversial. Fatkin¹² studied 11 families with autosomal dominant DCM with conduction defect and identified five *LMNA*-mutated DCM families (45%). Similarly, *LMNA*-mutated DCM was found in four of 49 families (8%) by Taylor,²⁰ two of 16 families (12.5%) by Jakobs,²¹ and five of seven (71%) families by Arbustini.²² Thus, the *LMNA* mutation may account for 19% of autosomal dominant DCM with conduction defect. Therefore, mutational analysis in *LMNA* should be first performed for the diagnosis of familial DCM associated with conduction defect.

Electrophysiological Characteristics

The first manifestation in the affected members was first- or second-degree AV block and/or AF, which developed at the mean age of 40 years (range 30-47 years). The EP study revealed AH block, that is, conduction defects in the AV node without those in the infra-Hisian conduction system. The PA interval, which may reflect the intraatrium conductivity, was within the normal range in affected members, IV-70 and V-65, but was prolonged in affected member V-69 whose diseased period had a long history (≥ 12 years).

Progressive AV block prior to LV dysfunction was unique in affected members with *LMNA*-mutated DCM. Some in-

vestigators have reported a similar time-course of *LMNA*-mutated DCM, that is, the conduction defect, including AV block and AF, developed prior to LV dysfunction,^{12,14,20-23} despite different sites of the mutation (Fig. 5). The present study indicated that the progressive AV block in *LMNA*-mutated DCM was caused by AV nodal impairment without infra-Hisian conduction defect.

AF frequently occurred in *LMNA*-mutated DCM.²⁴ However, AF may not be a particular phenotype of *LMNA* mutations, because LV dysfunction frequently causes AF. It remains unclear how *LMNA* and its locus, chromosome 1p1-q21, is related to familial AF.²⁵⁻²⁹

Sudden death accounted for 36% (5/14) of all causes of mortality in the *LMNA*-mutated DCM. Sudden death could not be prevented by PMI, and fatal VT appeared to cause sudden death. In fact, VT could be repeatedly induced by electrical stimulations of the RV in two affected members (V-65 and V-69). Affected member V-69 had spontaneous VT, and affected member V-65 developed spontaneous VT after the EP study. However, the incidence of sudden death is nearly identical to that of patients with DCM (approximately 40%).³⁰ Therefore, the susceptibility to VT and/or sudden deaths might not be specific to *LMNA*-mutated DCM; rather, it might be a common clinical feature of chronic heart failure with LV dysfunction.^{31,32}

Histopathological Characteristics

The microscopical study revealed that fibrosclerotic degeneration occurred predominantly in the AV node. Less severe lesions were also observed in the sinoatrial node, atrium, and ventricular walls. These supported the findings of the clinical examination and EP study that the AV block preceded the other myocardial involvements. The electron microscopical study revealed the accumulation of glycogen deposits beneath the subsarcolemma in the working myocardium in all biopsy samples.

Arbustini²² reported the fibrosclerotic and fibrofatty degeneration of the AV junction in *LMNA*-mutated DCM with conduction defect, and described the nuclear membrane damage showed by electron microscopical analysis.²² Lamin A and lamin C null mice also showed obvious discontinuities in the nuclear envelopes of embryonic fibroblasts and hepatocytes, while those of wild-type and heterozygous mice were intact.³³ However, electron microscopical study in the present report revealed that the nuclear membrane remained intact. This may be related to the sampling

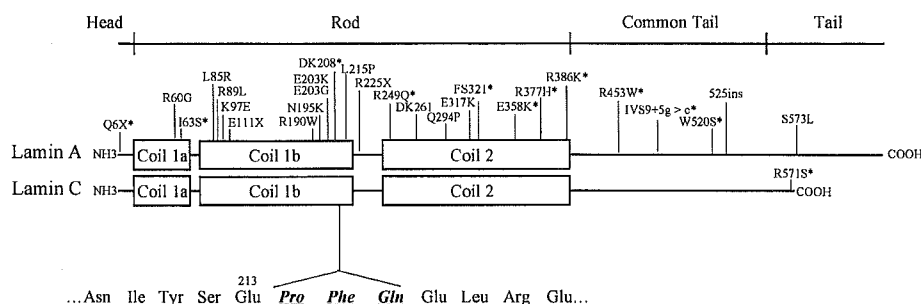


Figure 5. Secondary structure of lamin A and lamin C proteins and sites of mutations of *LMNA*-mutated DCM with conduction defect with or without muscular dystrophy. Secondary structure of lamin A and lamin C proteins is illustrated. The previously reported *LMNA* mutations (above) and the mutation identified in this study (below) as the cause of the DCM with conduction defect are shown. Asterisks indicate cases with skeletal muscle symptoms. Amino acids with bold and italic indicate the insertions those identified in this study.

site, that is, our biopsy samples were taken from the right ventricle.

Recently, it was reported that mutations in the gene coding the γ^2 regulatory subunit of AMP-activated protein kinase (*PRKAG2*), an enzyme that modulates glucose uptake and glycolysis, cause glycogen storage disease associated with cardiac hypertrophy and conduction defect including AV block.^{34,35} Therefore, we may be able to propose the hypothesis that the *LMNA* mutation causes cellular damage by the intracellular accumulation of glycogen. However, it remains unknown whether a dysfunction of lamin A and lamin C proteins impairs glycogen metabolism. Some types of familial diseases preferentially develop cardiac conduction defects even with a heterogenous genetic background.^{27,36,37} Understanding the actual molecular mechanism involved in the pathophysiology of familial diseases might enable us to understand the mechanisms of "common" cardiac conduction defects clinically recognized as "sporadic."

Conclusion

This is the first report of the electrophysiological profile of the progressive intra-AV nodal conduction impairment and its histopathological findings in *LMNA*-mutated DCM. The clinical phenotype of *LMNA*-mutated DCM in this study was characterized by (1) the first manifestation of the prolonged PQ interval or AF in adolescence, (2) progressive intra AV nodal block to the third degree in several years, and (3) progressive heart failure after PMI. Histological study revealed the preferential degeneration at the AV node area and novel cellular damages in the working myocardium.

Acknowledgments: We are grateful to the families who participated in this work. We also thank Ms. Kumi Kato and Ms. Shizue Mochizuki for technical assistance.

References

- McKeon FD, Kirschner MW, Caput D: Homologies in both primary and secondary structure between nuclear envelope and intermediate filament proteins. *Nature* 1986;319:463-468.
- Fisher DZ, Chaudhary N, Blobel G: cDNA sequencing of nuclear lamins A and C reveals primary and secondary structural homology to intermediate filament proteins. *Proc Natl Acad Sci USA* 1986;83:6450-6454.
- Stuurman N, Heins S, Aebi U: Nuclear lamins: Their structure, assembly, and interactions. *J Struct Biol* 1998;122:42-66.
- Wilson KL, Zastrow MS, Lee KK: Lamins and disease: Insights into nuclear infrastructure. *Cell* 2001;104:647-650.
- Bonne G, Di Barletta MR, Varnous S, Becane HM, Hammouda EH, Merlini L, Muntoni F, Greenberg CR, Gary F, Urtizberea JA, Duboc D, Fardeau M, Toniolo D, Schwartz K: Mutations in the gene encoding lamin A/C cause autosomal dominant Emery-Dreifuss muscular dystrophy. *Nat Genet* 1999;21:285-288.
- Raffaële Di Barletta M, Ricci E, Galluzzi G, Tonali P, Mora M, Morandi L, Romorini A, Voit T, Orstavik KH, Merlini L, Trevisan C, Biancalana V, Housmanowa-Petrusewicz I, Bione S, Ricotti R, Schwartz K, Bonne G, Toniolo D: Different mutations in the *LMNA* gene cause autosomal dominant and autosomal recessive Emery-Dreifuss muscular dystrophy. *Am J Hum Genet* 2000;66:1407-1412.
- Muchir A, Bonne G, van der Kooij AJ, van Meegen M, Baas F, Bolhuis PA, de Visser M, Schwartz K: Identification of mutations in the gene encoding lamins A/C in autosomal dominant limb girdle muscular dystrophy with atrioventricular conduction disturbances (LGMD1B). *Hum Mol Genet* 2000;9:1453-1459.
- Shackleton S, Lloyd DJ, Jackson SN, Evans R, Niermeijer MF, Singh BM, Schmidt H, Brabant G, Kumar S, Durrington PN, Gregory S, O'Rahilly S, Trembath RC: *LMNA*, encoding lamin A/C, is mutated in partial lipodystrophy. *Nat Genet* 2000;24:153-156.
- De Sandre-Giovannoli A, Chaouch M, Kozlov S, Vallat JM, Tazir M, Kassouri N, Szepletowski P, Hammadouche T, Vandenberghe A, Stewart CL, Grid D, Levy N: Homozygous defects in *LMNA*, encoding lamin A/C nuclear-envelope proteins, cause autosomal recessive axonal neuropathy in human (Charcot-Marie-Tooth disorder type 2) and mouse. *Am J Hum Genet* 2002;70:726-736.
- Novelli G, Muchir A, Sangiuolo F, Helbling-Leclerc A, D'Apice MR, Massart C, Capon F, Sbraccia P, Federici M, Lauro R, Tudisco C, Palotta R, Scarano G, Dallapiccola B, Merlini L, Bonne G: Mandibuloacral dysplasia is caused by a mutation in *LMNA*-encoding lamin A/C. *Am J Hum Genet* 2002;71:426-431.
- Eriksson M, Brown WT, Gordon LB, Glynn MW, Singer J, Scott L, Erdos MR, Robbins CM, Moses TY, Berglund P, Dutra A, Pak E, Durkin S, Csoka AB, Boehnke M, Glover TW, Collins FS: Recurrent de novo point mutations in lamin A cause Hutchinson-Gilford progeria syndrome. *Nature* 2003;423:293-298.
- Fatkin D, MacRae C, Sasaki T, Wolff MR, Porcu M, Frenneaux M, Atherton J, Vidaillet HJ, Jr., Spudich S, De Girolami U, Seidman JG, Seidman C, Muntoni F, Muehle G, Johnson W, McDonough B: Missense mutations in the rod domain of the lamin A/C gene as causes of dilated cardiomyopathy and conduction-system disease. *N Engl J Med* 1999;341:1715-1724.
- van der Kooij AJ, Ledderhof TM, de Voogt WG, Res CJ, Bouwsma G, Troost D, Busch HF, Becker AE, de Visser M: A newly recognized autosomal dominant limb girdle muscular dystrophy with cardiac involvement. *Ann Neurol* 1996;39:636-642.
- Becane HM, Bonne G, Varnous S, Muchir A, Ortega V, Hammouda EH, Urtizberea JA, Lavergne T, Fardeau M, Eymard B, Weber S, Schwartz K, Duboc D: High incidence of sudden death with conduction system and myocardial disease due to lamins A and C gene mutation. *Pacing Clin Electrophysiol* 2000;23:1661-1666.
- Kure S, Takayanagi M, Narisawa K, Tada K, Leisti J: Identification of a common mutation in Finnish patients with nonketotic hyperglycinemia. *J Clin Invest* 1992;90:160-164.
- Josephson ME. *Clinical Cardiac Electrophysiology: Techniques and Interpretations*. Malvern: Lea&Febiger, 1993: p. 437.
- Freedman RA, Swerdlow CD, Echt DS, Winkle RA, Soderholm-Difatte V, Mason JW: Facilitation of ventricular tachyarrhythmia induction by isoproterenol. *Am J Cardiol* 1984;54:765-770.
- Bonne G, Mercuri E, Muchir A, Urtizberea A, Becane HM, Recan D, Merlini L, Wehnert M, Boor R, Reuner U, Vorgerd M, Wicklein EM, Eymard B, Duboc D, Penisson-Besnier I, Cuisset JM, Ferrer X, Desguerre I, Lacombe D, Bushby K, Pollitt C, Toniolo D, Fardeau M, Schwartz K, Muntoni F: Clinical and molecular genetic spectrum of autosomal dominant Emery-Dreifuss muscular dystrophy due to mutations of the lamin A/C gene. *Ann Neurol* 2000;48:170-180.
- Garg A, Speckman RA, Bowcock AM: Multisystem dystrophy syndrome due to novel missense mutations in the amino-terminal head and alpha-helical rod domains of the lamin A/C gene. *Am J Med* 2002;112:549-555.
- Taylor MR, Fain PR, Sinagra G, Robinson ML, Robertson AD, Carniel E, Di Lenarda A, Bohlmeier TJ, Ferguson DA, Brodsky GL, Boucek MM, Lascor J, Moss AC, Li WL, Stetler GL, Muntoni F, Bristow MR, Mestroni L: Natural history of dilated cardiomyopathy due to lamin A/C gene mutations. *J Am Coll Cardiol* 2003;41:771-780.
- Jakobs PM, Hanson EL, Crispell KA, Toy W, Keegan H, Schilling K, Icenogle TB, Litt M, Hershberger RE: Novel lamin A/C mutations in two families with dilated cardiomyopathy and conduction system disease. *J Card Fail* 2001;7:249-256.
- Arbustini E, Pilotto A, Repetto A, Grasso M, Negri A, Diegoli M, Campana C, Scelsi L, Baldini E, Gavazzi A, Tavazzi L: Autosomal dominant dilated cardiomyopathy with atrioventricular block: A lamin A/C defect-related disease. *J Am Coll Cardiol* 2002;39:981-990.
- Hershberger RE, Hanson EL, Jakobs PM, Keegan H, Coates K, Bousman S, Litt M: A novel lamin A/C mutation in a family with dilated cardiomyopathy, prominent conduction system disease, and need for permanent pacemaker implantation. *Am Heart J* 2002;144:1081-1086.
- Sebillon P, Bouchier C, Bidot L, Bonne G, Ahamed K, Charron P, Drouin-Garraud V, Millaire A, Desrumaux G, Benaiche A, Charniot JC, Schwartz K, Villard E, Komajda M: Expanding the phenotype of *LMNA* mutations in dilated cardiomyopathy and functional consequences of these mutations. *J Med Genet* 2003;40:560-567.
- Olson TM, Keating MT: Mapping a cardiomyopathy locus to chromosome 3p22-p25. *J Clin Invest* 1996;97:528-532.
- Brugada R, Tapscott T, Czernuszewicz GZ, Marian AJ, Iglesias A, Mont L, Brugada J, Girona J, Domingo A, Bachinski LL, Roberts R:

- Identification of a genetic locus for familial atrial fibrillation. *N Engl J Med* 1997;336:905-911.
27. Chen YH, Xu SJ, Bendahhou S, Wang XL, Wang Y, Xu WY, Jin HW, Sun H, Su XY, Zhuang QN, Yang YQ, Li YB, Liu Y, Xu HJ, Li XF, Ma N, Mou CP, Chen Z, Barhanin J, Huang W: KCNQ1 gain-of-function mutation in familial atrial fibrillation. *Science* 2003;299:251-254.
 28. Darbar D, Herron KJ, Ballew JD, Jahangir A, Gersh BJ, Shen WK, Hammill SC, Packer DL, Olson TM: Familial atrial fibrillation is a genetically heterogeneous disorder. *J Am Coll Cardiol* 2003;41:2185-2192.
 29. Ellinor PT, Shin JT, Moore RK, Yoerger DM, MacRae CA: Locus for atrial fibrillation maps to chromosome 6q14-16. *Circulation* 2003;107:2880-2883.
 30. Koseki Y, Watanabe J, Shinozaki T, Sakuma M, Komaru T, Fukuchi M, Miura M, Karibe A, Kon-No Y, Numaguchi H, Ninomiya M, Kagaya Y, Shirato K, The CI: Characteristics and 1-year prognosis of medically treated patients with chronic heart failure in Japan. *Circ J* 2003;67:431-436.
 31. Stevenson WG, Sweeney MO: Arrhythmias and sudden death in heart failure. *Jpn Circ J* 1997;61:727-740.
 32. Huikuri HV, Castellanos A, Myerburg RJ: Sudden death due to cardiac arrhythmias. *N Engl J Med* 2001;345:1473-1482.
 33. Sullivan T, Escalante-Alcalde D, Bhatt H, Anver M, Bhat N, Nagashima K, Stewart CL, Burke B: Loss of A-type lamin expression compromises nuclear envelope integrity leading to muscular dystrophy. *J Cell Biol* 1999;147:913-920.
 34. Arad M, Benson DW, Perez-Atayde AR, McKenna WJ, Sparks EA, Kanter RJ, McGarry K, Seidman JG, Seidman CE: Constitutively active AMP kinase mutations cause glycogen storage disease mimicking hypertrophic cardiomyopathy. *J Clin Invest* 2002;109:357-362.
 35. Gollob MH, Green MS, Tang AS, Gollob T, Karibe A, Ali Hassan AS, Ahmad F, Lozado R, Shah G, Fananapazir L, Bachinski LL, Roberts R, Hassan AS: Identification of a gene responsible for familial Wolff-Parkinson-White syndrome. *N Engl J Med* 2001;344:1823-1831.
 36. Goldfarb LG, Park KY, Cervenakova L, Gorokhova S, Lee HS, Vasconcelos O, Nagle JW, Semino-Mora C, Sivakumar K, Dalakas MC: Missense mutations in desmin associated with familial cardiac and skeletal myopathy. *Nat Genet* 1998;19:402-403.
 37. Schott JJ, Alshinawi C, Kyndt F, Probst V, Hoorntje TM, Hulsbeek M, Wilde AA, Escande D, Mannens MM, Le Marec H: Cardiac conduction defects associate with mutations in SCN5A. *Nat Genet* 1999;23:20-21.

Avihu Boneh · Stanley H. Korman · Kenichi Sato
Junko Kanno · Yoichi Matsubara · Israella Lerer
Ziva Ben-Neriah · Shigeo Kure

A single nucleotide substitution that abolishes the initiator methionine codon of the *GLDC* gene is prevalent among patients with glycine encephalopathy in Jerusalem

Received: 12 January 2005 / Accepted: 23 February 2005 / Published online: 29 April 2005
© The Japan Society of Human Genetics and Springer-Verlag 2005

Abstract Glycine encephalopathy (GE) (non-ketotic hyperglycinemia) is an autosomal recessive neurometabolic disease caused by defective activity of the glycine cleavage system. Clinically, patients present usually in the neonatal period with hypotonia, encephalopathy, hiccups and breath arrests with or without overt seizures. GE is considered rare, but its incidence is relatively high in several geographical areas around the world. We report a novel mutation causing GE in six extended Arab families, all from a small suburban village (population 5,000). A methionine to threonine change in the initiation codon of the glycine decarboxylase gene led to markedly reduced glycine decarboxylase mRNA levels and abolished glycine cleavage system activity.

Keywords Glycine encephalopathy · Non-ketotic hyperglycinemia · Glycine decarboxylase · Mutation · Initiation codon

A. Boneh · I. Lerer · Z. Ben-Neriah
Department of Human Genetics,
Hadassah-Hebrew University Medical Centre,
Jerusalem, Israel

S. H. Korman
Department of Clinical Biochemistry,
Hadassah-Hebrew University Medical Centre,
Jerusalem, Israel

K. Sato · J. Kanno · Y. Matsubara · S. Kure
Department of Medical Genetics,
Tohoku University School of Medicine,
Sendai, Japan

A. Boneh (✉)
Metabolic Service, Genetic Health Services Victoria,
The Murdoch Children's Research Institute,
Royal Children's Hospital, Flemington Road,
Melbourne, Victoria, 3052 Australia
E-mail: avihu.boneh@ghsv.org.au
Tel.: +61-3-83416252
Fax: +61-3-83416390

Introduction

Glycine encephalopathy (GE; or non-ketotic hyperglycinemia, OMIM 238300) is an autosomal recessive neurometabolic disease caused by defective activity of the glycine cleavage system (Hamosh and Johnston 2001). This complex is made of four proteins that work in concert in the metabolic process of glycine: a P protein, a pyridoxal-phosphate-containing glycine decarboxylase (GLDC), a T protein, a tetrahydrofolate requiring aminomethyltransferase, an L protein, a lipamide dehydrogenase and a lipoic-acid-containing H protein. The P protein, T protein and H protein are encoded by the *GLDC*, *AMT* and *GCSH* genes, respectively. Defects in the P protein, the GLDC, are the most common causes of GE and lead to more than 80% of GE cases.

Classical GE typically presents in the first days of life. Assisted ventilation is needed to overcome severe and prolonged apnoeic episodes with or without overt seizures. Babies present also with hypotonia, lethargy and hiccups. Most children who survive the neonatal period are severely disabled. Despite the almost universally similar clinical outcome of the disorder, the number of disease-causing mutations in the genes encoding the P and the T proteins is steadily growing, and a clear genotype-phenotype correlation is not possible at this stage.

The GE is considered rare, but its prevalence is relatively high in several geographical areas around the world (von Wendt et al. 1979; Kure et al. 1998; Applegarth et al. 2000). In the last 15 years, we have been treating several children with GE from six Arab families from a suburban village near Jerusalem. Some of these children have been previously reported (Boneh et al. 1996). We report the finding of a single mutation in the initiation codon of the P protein causing GE in all these families.

Patients and methods

Patients

We analysed DNA samples from 31 individuals from six families, including eight patients (Table 1). The parents of patients in five families were first cousins (Fig. 1). The parents in family 4 were unrelated but originated from families 1 and 2. Five of these patients (families 1 and 3) have been previously reported (Boneh et al. 1996). All patients except one presented with hypotonia and respiratory abnormalities on days 3–4 of life, followed in all patients by apnoea, poor reflexes and, in three patients, hiccups. Seizures were not a prominent feature of their initial clinical presentation, but some patients had seizures later. Patient III:1 and patient III:4, both from family 2, deceased at 14 and 9 years of age, respectively. The patient in family 5 (patient 1), a female, fed poorly and did not wake up for feeds on day 2 of life, and when hospitalised on day 3, she was markedly hypotonic and did not awaken even in response to painful stimuli. Primitive reflexes could not be elicited. Convulsions were observed on day 4. Neither apnoea nor hiccups were noted at any stage. CSF and plasma glycine levels were

Table 1 The *GLDC* MIT mutation in six glycine encephalopathy (GE) families in Jerusalem

Family	Member	Genotype
Family 1	III:2	Heterozygote
	III:4	Heterozygote
	IV:1	Heterozygote
	IV:2	Heterozygote
	IV:3	Heterozygote
	IV:4	Heterozygote
	IV:5	Heterozygote
	V:1	No mutant allele
V:2	No mutant allele	
V:3 (proband)	Homozygote	
V:5	Homozygote	
V:4	No mutant allele	
Family 2	II:1	Heterozygote
	II:2	Heterozygote
	III:1 (proband)	Homozygote
	III:2	Heterozygote
	III:3	Heterozygote
	III:4	Homozygote
	III:6	Heterozygote
	III:7	Heterozygote
Family 3	IV:1	Homozygote
	Father	Heterozygote
	Mother	Heterozygote
	Brother	Heterozygote
Family 4	Patient	Not determined
	Father	Heterozygote
	Mother	Heterozygote
Family 5	Patient	Homozygote
	Father	Heterozygote
	Mother	Heterozygote
Family 6	Patient	Homozygote
	Father	Not determined
	Mother	Not determined
	Patient	Homozygote

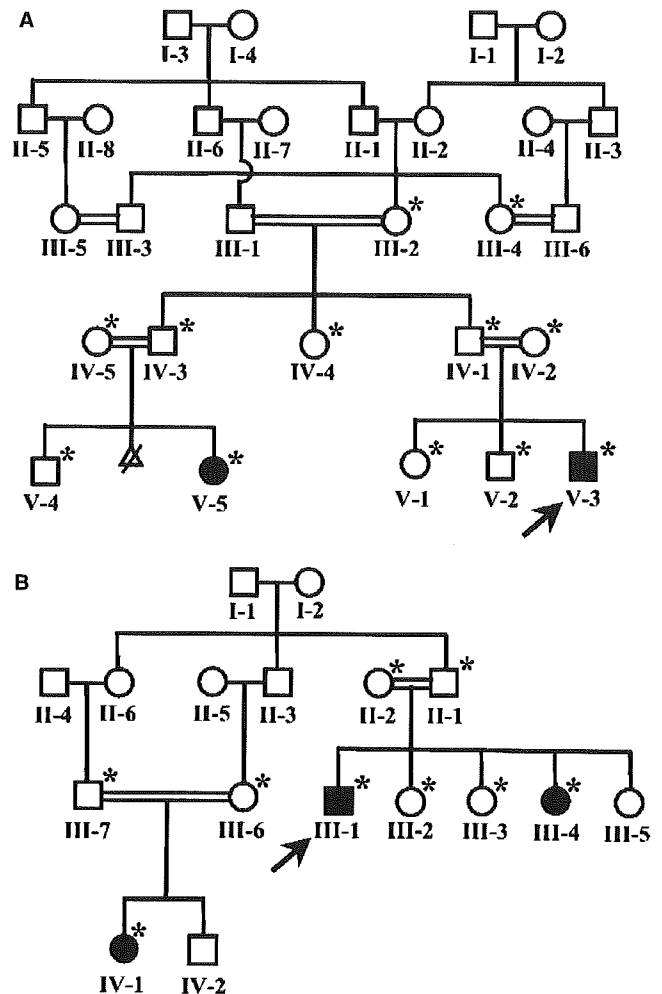


Fig. 1 Family trees of families 1 and 2 are shown. Note consanguinity. Asterisks denote individuals from whom DNA was analysed. The probands in both families are marked with an arrow

119 and 808 $\mu\text{mol/l}$, respectively, with a ratio of 0.15. The patient in family 6 (patient 2), a male, was noted to be sleepy, not crying, flaccid and sucking poorly on day 2 of life. On day 3, CSF and plasma glycine levels were 210 and 2,187, respectively, with a ratio of 0.10. He required mechanical ventilation but later regained spontaneous respiration and resumed oral feeding. He has not had seizures. Although he seemed to develop normally in the first months of life, at 18 months of age, he had axial hypotonia, could not walk and said single syllables but no words. He had not had seizures. All other patients were severely disabled.

Sequencing analysis

We have amplified 25 exons of the *GLDC* gene by PCR, as described (Takayanagi et al. 2000), as well as nine exons of the *AMT* gene and five exons of the *GCSH* gene. Exon Amplicons were subjected to 2.5% agarose gel electrophoresis, and bands with the expected size

were cut out for DNA purification. Nucleotide sequences were determined by the dye-terminator cycle sequencing kit (PE biosystems, Foster City, CA, USA) using the PE1F primer as a sequencing primer.

Multiplex RT-PCR analysis

Lymphoblast cell lines were established from two patients: patient II:1 from family 5 (patient 1) and patient I:1 from family 6 (patient 2). Total RNA was prepared from each cell line, and 10 µg of each was used for reverse transcription in 20 µl of mixture, as described (Kure et al. 1992b). GLDC cDNA fragment with 600 bp was amplified with a set of primers GLDC-D1, 5'-TGGCCAAGCGATTAGAAACACACT-3'; GLDC-D2, 5'-TATCAAATGCTCTGGGGAGAGGCAT-3' while LPT cDNA fragment (772 bp) was amplified by a pair of PCR primers using LPT21F, 5'-AG-GCGCCCGCACCACGCCCA-3'; LPT17R, 5'-TCCTGATCCCTGGTAAGGGCTC-3'. Both PCRs was performed in a single tube (30 µl of PCR mix) using Multiplex PCR Kit (Qiagen, Germany) according to the manufacturer's protocol. A total of 2 µl of reverse transcription mixtures was subjected to multiplex PCR analysis, and 10 µl of PCR products were size-separated on 2.5% agarose gel electrophoresis. The intensity of each band and the ratio of the GLDC/LPT bands were calculated by the NIH Image software.

Assay of the glycine cleavage system activity in lymphoblasts

Enzymatic activity of the glycine cleavage system in lymphoblast cell lines (patients 1 and 2) was determined by the decarboxylation reaction using [$1-^{14}C$]glycine, as described (Kure et al. 1992a). The assay was performed in triplicate, and means and standard deviations were determined.

Results

Identification of the MIT mutation in GLDC exon 1

We screened the *GLDC*, *AMT* and *GCSH* genes for mutations using DNA obtained from the proband in family 1 (patient V:3). A homozygous single-base substitution from T to C (c.2T > C) was found in exon 1 of the *GLDC* gene. This substitution changes the obligate/consensus initiation ATG codon (encoding methionine) to ACG (normally encoding threonine) and is hence termed the MIT mutation, as shown in Fig. 2. The parents of the proband were heterozygous for this mutation. The MIT mutation was then screened for in all six families with GE from this village and was detected in all of them. The results of the genotyping are shown in Table 1. All patients in these families were

homozygous for the MIT mutation while all obligate carriers were heterozygous for the mutation. A total of 122 control alleles from the same population were analysed, and no MIT mutant allele was identified in these DNA samples.

Expression of the mutant transcripts

We considered the possibility that the mutant *GLDC* mRNA would be unstable by a mechanism of nonsense-mediated mRNA decay because the MIT mutation abolished the initiator codon. To examine the level of the *GLDC* mRNA expressed in lymphoblasts, we performed a multiplex RT-PCR analysis using *LPT* mRNA as a control. The *LPT* gene encodes a housekeeping enzyme, lipoyl transferase, that generates holo-H-protein by conjugating lipoic acid to apo-H-protein (Fujiwara et al. 1999). Both cDNA fragments, derived from *LPT* and *GLDC* genes, were successfully amplified in a single reaction mixture (Fig. 3). Ratios of cDNA band intensity (*GLDC*/*LPT*) were calculated to be 0.95, 1.12, 0.14 and 0.08 in control 1, control 2, patient 1 and patient 2 lymphoblast cell lines, respectively, indicating that *GLDC* mRNA levels were markedly reduced in the tested patients' cell lines.

Glycine cleavage system activity in lymphoblasts

Glycine decarboxylation activity of lymphoblasts was 0.1 ± 0.20 and 0 ± 0.15 (normal range 0.61–16) nmole of

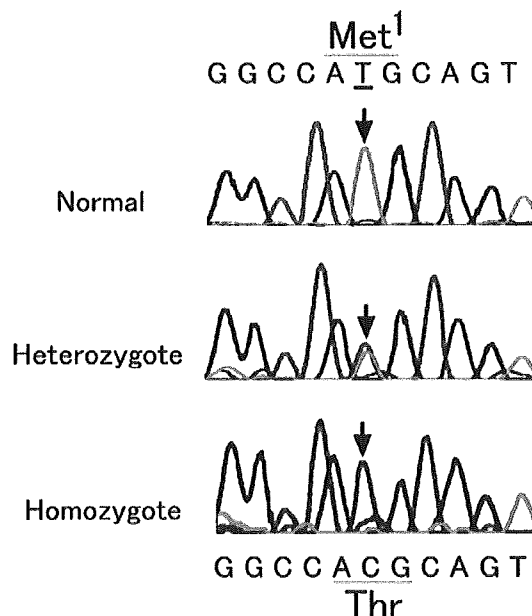


Fig. 2 Sequencing chromatogram of the MIT mutation. PCR fragments containing *GLDC* exon 1 were amplified from genomic DNA from a control subject, an obligate heterozygote and a patient, and was sequenced by the dye-terminator method. The MIT mutation sites are indicated by arrows

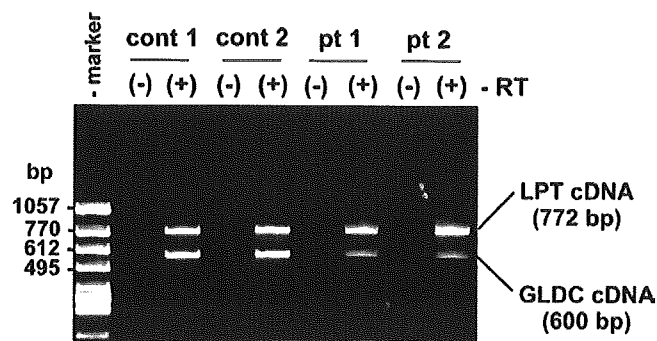


Fig. 3 Multiplex RT-PCR analysis of GLDC mRNA expressed in patients' lymphoblasts. Total RNA samples were prepared from two control subjects (*cont 1 and 2*) and two patients (*pt 1 and 2*) and subjected to reverse transcription and multiplex PCR (*RT + lanes*). As a negative control, the same amount of total RNA was used for multiplex PCR amplification without reverse transcription (*RT - lanes*)

$^{14}\text{CO}_2$ -formed/mg protein/h in patients 1 and 2 lymphoblast cells, respectively, indicating that the enzyme activity was completely abolished in these patients.

Discussion

GE is a rare disorder, but its exact world-wide incidence is not known. A high incidence of GE has been reported in certain ethnic groups and geographical locations. In Finland, the incidence of GE is 1 in 55,000 new-born babies, but it is even higher in northern Finland, with an incidence of 1 in 12,000 (von Wendt et al. 1979). The incidence of GE in British Columbia, Canada, is 1 in 63,000, also probably higher than the expected world-wide incidence (Applegarth et al. 2000). A high incidence of GE has been previously reported in an Arab village in Israel (Kure et al. 1998). Moreover, single mutations have been reported as a cause of GE in some of these populations. Thus, a single mutation, Ser564Ile, has been found to be the cause of the high incidence of GE in Finland (Kure et al. 1992b). Likewise, a single mutation in the T protein, His42Arg, was found to be the cause of the high incidence in the Arab village in northern Israel (Kure et al. 1998).

The current report adds to the list of single mutations leading to a high incidence of GE in isolated populations. A single novel mutation caused GE in eight patients (and one deceased proband from whom no DNA was available for analysis) from six families, all from a small geographical area near Jerusalem. The inhabitants of this suburban village (approximately 5,000 people) live as large kindreds, as is common to many communities in this geographical area (Jaber et al. 2000; Zlotogora et al. 1996) (for example, see Fig. 1). Consanguinity in this population is common and has been estimated at ~33% of all marriages (Jaber et al. 2000). Interestingly, DNA analysis of another family from a different area near Jerusalem revealed another

causative mutation (Korman et al. 2004). Thus, based on the theoretical calculations presented previously (Zlotogora et al. 1996), it may be surmised that the mutation reported here occurred around five generations ago.

Mutations affecting the ATG start codon have not been widely reported. In theory, there are several potential consequences of such mutations, ranging from a near-normal protein product to a complete absence of the protein or a truncated protein, the extent of which being dependent on the location of the next ATG sequence.

It has been suggested that initiation codons are recognised most efficiently when they are located in a favourable context, as defined by the Kozak consensus sequence ACCatgG (Kozak 1986). Different permutations of non-ATG codons have varying capacities to substitute as initiation codons, but their efficiency is questionable. Indeed, our results indicate that the mRNA level was reduced in the patients' cell lines.

The mechanism by which a moderate reduction of the level of the mutant mRNA leads to severe dysfunction of the gene product remains unknown. Given that our patients had null GCS activity in the enzymatic analysis, one would have expected the level of the GLDC mRNA to be very low or negligible if one would attribute the null activity to the level of the GLDC mRNA only. However, although the level of GLDC mRNA in the RT-PCR analysis was markedly reduced, it was not negligible, suggesting that the reduction of the GLDC mRNA was not the primary or only cause of null enzymatic activity. One possible explanation for this finding is that lack of recognition of the first initiator methionine by the translation complex may lead to instability of the mutant GLDC mRNA. Further analysis using *in vitro* expression of mutant GLDC RNA is required to elucidate this possibility.

The other possible mechanism relates to the targeting of the gene product to the mitochondria. The next ATG codon in the GLDC gene at which translation could initiate is located 231 nucleotides downstream. It is situated in-frame in a partially favourable context (GAGAGatgCT). Use of this codon for initiation of translation would result in deletion of 77 amino acid residues with loss of the mitochondrial leader peptide. The GLDC is a component of the multi-enzyme system that operates in mitochondria in concert with three other GCS components. Thus, it may be predicted that as a result of the MIT mutation, which abolished the initiator methionine and could be expected to lead to the truncation of the mitochondrial leader peptide of the GLDC precursor, the mutant GLDC would not enter into the mitochondria nor interact with other GCS components. This would render the protein product non-functional and may provide another explanation to the null GCS activity in the lymphoblast cell line and severe symptoms of the homozygous patients.

An initiation codon mutation was also reported in the ornithine delta aminotransferase, causing gyrate atrophy

of the choroid and retina (Mitchell et al. 1988). As in our patients, the protein product of the mutated gene was expected to truncate 138 amino acids of the ornithine amino transferase enzyme, thus eliminating the entire mitochondrial leader sequence and abolishing enzyme activity (Mitchell et al. 1988). Likewise, Frank et al. (1999) reported two mutations in the initiation codon of the protoporphyrinogen oxidase gene, leading to variegate porphyria due to a non-functional protein. By contrast, a mutation in the translation initiation codon of the mitochondrial acetoacetyl-CoA thiolase gene did not affect the gene-product mRNA levels and did not completely abolish enzyme activity, yielding a residual activity of 15% (Fukao et al. 2003). Cremonesi et al. (2004) have reported a mutation in the ATG initiation codon of the L-ferritin gene that disabled protein expression but did not cause iron deposition in the brain and did not lead to any haematological or neurological symptoms. Moreover, mutations in the ATG initiation codon have also been shown to be markers of common haplotypes. For example, the mitochondrial T3308C mutation in the initiation codon of the NADH-dehydrogenase subunit 1 seems to be an ancient marker of a common West African haplogroup (Rocha et al. 1999). Likewise, in a large phylogeographic analysis of mitochondrial DNA haplogroups in China, the T12338C mutation in the initiation codon of the NADH-dehydrogenase subunit 5 was shown to be a common polymorphic change in various populations across China (Kong et al. 2004). It seems, therefore, that mutations in the translation initiation codon do not necessarily cause a severe deficiency of the gene product, and the effects of these mutations need to be evaluated specifically for each gene, as previously suggested (Fukao et al. 2003).

In summary, we have found a novel mutation, M1T, in the initiation codon of the glycine carboxylase gene, leading to reduced RNA levels, abolished enzyme activity and clinical evidence of GE in several families from a small geographical area. The identification of a common mutation in this population is of significance in that it will enable fast, easy and reliable genetic screening and prenatal diagnosis for interested couples in this community in the future.

References

- Applegarth DA, Toone JR, Lowry RB (2000) Incidence of inborn errors of metabolism in British Columbia, 1969–1996. *Pediatrics* 105:e10
- Boneh A, Degani Y, Harari M (1996) Prognostic clues and outcome of early treatment of nonketotic hyperglycinemia. *Pediatr Neurol* 15:137–141
- Cremonesi L, Cozzi A, Girelli D, Ferrari F, Fermo I, Foglieni B, Levi S, Bozzini C, Camparini M, Ferrari M, Arosio P (2004) Case report: a subject with a mutation in the ATG start codon of L-ferritin has no haematological or neurological symptoms. *J Med Genet* 41:e81
- Frank J, McGrath JA, Poh-Fitzpatrick MB, Hawk JL, Christiano AM (1999) Mutations in the translation initiation codon of the protoporphyrinogen oxidase gene underlie variegate porphyria. *Clin Exp Dermatol* 24:296–301
- Fujiwara K, Suzuki M, Okumachi Y, Okamura-Ikeda K, Fujiwara T, Takahashi E, Motokawa Y (1999) Molecular cloning, structural characterization and chromosomal localization of human lipoyltransferase gene. *Eur J Biochem* 260:761–767
- Fukao T, Matsuo N, Zhang GX, Urasawa R, Kubo T, Kohno Y, Kondo N (2003) Single base substitutions at the initiator codon in the mitochondrial acetoacetyl-CoA thiolase (ACAT1/T2) gene result in production of varying amounts of wild-type T2 polypeptide. *Hum Mutat* 21:587–592
- Hamosh A, Johnston MV (2001) Non-ketotic hyperglycinemia. In: Scriver CRBA, Sly WS, Valle D, (eds) *The metabolic and molecular bases of inherited disease*. McGraw-Hill, New York, pp2065–2078
- Jaber L, Halpern GJ, Shohat T (2000) Trends in the frequencies of consanguineous marriages in the Israeli Arab community. *Clin Genet* 58:106–110
- Kong QP, Yao YG, Sun C, Zhu CL, Zhong L, Wang CY, Cai WW, Xu XM, Xu AL, Zhang YP (2004) Phylogeographic analysis of mitochondrial DNA haplogroup F2 in China reveals T12338C in the initiation codon of the ND5 gene not to be pathogenic. *J Hum Genet* 49:414–423
- Korman SH, Boneh A, Ichinohe A, Kojima K, Sato K, Ergaz Z, Gomori JM, Gutman A, Kure S (2004) Persistent NKH with transient or absent symptoms and a homozygous GLDC mutation. *Ann Neurol* 56:139–143
- Kozak M (1986) Point mutations define a sequence flanking the AUG initiator codon that modulates translation by eukaryotic ribosomes. *Cell* 44:283–292
- Kure S, Narisawa K, Tada K (1992a) Enzymatic diagnosis of nonketotic hyperglycinemia with lymphoblasts. *J Pediatr* 120:95–98
- Kure S, Takayanagi M, Narisawa K, Tada K, Leisti J (1992b) Identification of a common mutation in Finnish patients with nonketotic hyperglycinemia. *J Clin Invest* 90:160–164
- Kure S, Mandel H, Rolland MO, Sakata Y, Shinka T, Drugan A, Boneh A, Tada K, Matsubara Y, Narisawa K (1998) A missense mutation (His42Arg) in the T-protein gene from a large Israeli-Arab kindred with nonketotic hyperglycinemia. *Hum Genet* 102:430–434
- Mitchell GA, Brody LC, Looney J, Steel G, Suchanek M, Dowling C, Der Kaloustian V, Kaiser-Kupfer M, Valle D (1988) An initiator codon mutation in ornithine-delta-aminotransferase causing gyrate atrophy of the choroid and retina. *J Clin Invest* 81:630–633
- Rocha H, Flores C, Campos Y, Arenas J, Vilarinho L, Santorelli FM, Torroni A (1999) About the “Pathological” role of the mtDNA T3308C mutation. *Hum Genet* 65:1457–1459
- Takayanagi M, Kure S, Sakata Y, Kurihara Y, Ohya Y, Kajita M, Tada K, Matsubara Y, Narisawa K (2000) Human glycine decarboxylase gene (GLDC) and its highly conserved processed pseudogene (psiGLDC): their structure and expression, and the identification of a large deletion in a family with nonketotic hyperglycinemia. *Hum Genet* 106:298–305
- von Wendt L, Hirvasniemi A, Simila S (1979) Nonketotic hyperglycinemia. A genetic study of 13 Finnish families. *Clin Genet* 15:411–417
- Zlotogora J, Gieselmann V, Bach G (1996) Multiple mutations in a specific gene in a small geographic area: a common phenomenon? *Am J Hum Genet* 58:241–243

Minireview

Atypical variants of nonketotic hyperglycinemia

Argirios Dinopoulos^{a,*}, Yoichi Matsubara^b, Shigeo Kure^b

^a Cincinnati Children's Hospital Medical Center, Division of Neurology, 3333 Burnet Avenue, Cincinnati, OH 45229-3039, USA

^b Department of Medical Genetics, Tohoku University School of Medicine, 1-1 Seiryomachi, Aobaku, Sendai 980-8574, Japan

Received 1 June 2005; received in revised form 26 July 2005; accepted 27 July 2005

Available online 12 September 2005

Abstract

Clinical symptoms in atypical nonketotic hyperglycinemia (NKH) are heterogeneous, in sharp contrast to uniform severe neurological symptoms in the classical NKH. A review of the literature of atypical NKH cases reveals three forms: *neonatal*, *infantile*, and *late onset*. The presentation in the *neonatal* form is similar to the classical one but the subsequent outcome is significantly better. Mental retardation and behavioral abnormalities are prevalent in both *infantile* and *late onset* forms although the phenotype in *late onset* atypical NKH is more heterogeneous. Patients with the atypical NKH tend to have a lower CSF/plasma glycine ratio when compared with the classical form, but overlap occurs. Hyperglycinemia in the *neonatal* and *infantile* atypical NKH, similar to the classical form, is caused by a deficient glycine cleavage system, whereas the cause of hyperglycinemia in *late onset* atypical NKH is unknown. A mutation of the T-protein *AMT* gene and several mutations of P-protein *GLDC* gene have been identified in homozygous or compound heterozygous state. Some of the *GLDC* mutations are associated with residual glycine decarboxylase activity when expressed in COS7 cells and early therapeutic intervention may be crucial to improve the outcome in patients harboring such mutations. Identification of more mutations causing atypical NKH and information about the mutations' effect on enzyme activity may help to predict patients with a milder phenotype as well as those who may respond to early therapeutic intervention.

© 2005 Elsevier Inc. All rights reserved.

Keywords: Atypical nonketotic hyperglycinemia; Mild glycine encephalopathy; Infantile NKH; Late onset NKH; *GLDC* mutations; Glycine decarboxylase activity

Introduction

Nonketotic hyperglycinemia (NKH) or glycine encephalopathy (GE) MIM 605899 is an autosomal recessive inborn error of glycine degradation in which large quantities of glycine accumulate in all body tissues, particularly in the central nervous system. The biochemical hallmark of NKH is increased glycine concentration in the plasma and, to an even greater extent, in the cerebrospinal fluid (CSF). The fundamental defect occurs in the glycine cleavage system (GCS), a multienzyme complex located in the inner mitochondrial membrane of the brain, liver, kidney, and placenta. This complex consists

of four individual protein components, termed P-protein (a pyridoxal phosphate-dependent glycine decarboxylase), H-protein (a lipoic acid-containing hydrogen carrier protein), T-protein (a tetrahydrofolate-dependent aminomethyltransferase), and L-protein (a lipoamide dehydrogenase), which are encoded by *GLDC*, *GCSH*, *AMT*, and *GCSL* genes, respectively. Previous genetic analysis of GCS revealed that the human P-protein gene (*GLDC*) consists of 25 exons on chromosome 9p22–24 [1], the T-protein gene (*AMT*) consists of nine exons on chromosome 3p21.1–21.2 [2], the H-protein gene (*GCSH*) consists of five exons on chromosome 16q24 [3], and the L-protein gene (*GCLS*) consists of 12 exons on chromosome 7q31–32 [4].

Classical NKH presents in the early neonatal period with progressive lethargy, feeding difficulty, hypotonia, myoclonic jerks, and apnea with most newborns

* Corresponding author. Fax: +1 513 6361888.

E-mail address: Agirios.Dinopoulos@cchmc.org, argidino@yahoo.com (A. Dinopoulos).

requiring assisted ventilation in the first week of life. Survivors almost invariably display profound neurological disability and intractable seizures. Enzymatic analysis suggests that most patients with classical NKH have deficient P-protein (80%) and T-protein (15%), and H-protein deficiency is rare [5]. With the exception of a common, founder effect mutation (S564I, G761R, and R515S) [6,7] in the *GLDC* gene among Finnish and Caucasian patients, there are few reports of recurring *GLDC* and *AMT* mutations [8], and most NKH patients are likely to be compound heterozygotes [9].

There are several reports of patients with biochemical, enzymatic, and genetic evidence of NKH but a less severe atypical presentation with variable age of onset. Atypical variants of NKH have been diagnosed in patients with rather disparate manifestations partially because the diagnosis of most cases was based on the plasma and CSF glycine concentration without the enzymatic or genetic confirmation. To clinically, biochemically, and genetically characterize the different forms of atypical NKH, a literature review was performed between the years of 1965 and 2005 in all ages.

Literature review

A MEDLINE search was performed of studies from the years 1965 to 2005, in all ages. Studies were reviewed in full and references of studies were also reviewed by hand to locate additional studies missed by the computer search. Data abstracted from eligible publications included age of onset, symptomatology, initial biochemical data (CSF glycine, plasma glycine, and CSF/plasma glycine ratio), enzymatic assays in liver or fibroblasts, other testing (glycine tolerance test, EEG, and brain imaging,) and therapeutic interventions. In the study were included cases with an NKH diagnosis based on abnormal CSF/plasma glycine level and/or enzymatic or genetic testing. Cases in which the diagnosis of NKH was based only on plasma glycine level were excluded. The type of the atypical NKH was labeled according to the age of the initial presentation (*neonatal*: 0–4 weeks, *infantile*: 5 weeks–2 years, and *late onset*: >2 years). The degree of cognitive impairment was rated, based on clinical information and, when possible according to a validated scale. *Normal* designates no cognitive impairment and normal IQ. *Mild* designates global and language delay but able to attend school (special education classes) and, overall, to live semi-independently, or IQ of >51 and <70. *Moderate to severe* indicates that they are completely dependant, or an IQ of <50 if reported. The CSF/plasma glycine ratio was the main biochemical marker, that was used because it is more specific for NKH and less prone to bias arising by comparing values from different laboratories. To identify whether there is an association between the met-

abolic defect and the phenotype, we measured the association between CSF/plasma glycine ratios and cognitive impairment—normal, mild, and moderate/severe—using the Kruskal Wallis *H* test.

Since the initial clinical and biochemical description of the disease [10], 50 patients (27 females and 23 males) in 32 sibships with an atypical presentation of NKH have been described in the literature (Table 1). In 31 of them the diagnosis was confirmed either by enzymatic essays on liver or lymphoblasts (11 patients) or by identification of a pathogenic mutation (20 patients). A P-protein defect was found by direct enzyme measurement in two patients and by a mutation on *GLDC* gene on 19 patients. Four patients in two sibships had a T-protein defect and five a decreased GCS activity with unidentifiable specific defect. In 18 patients the diagnosis was based on increased CSF glycine/plasma glycine ratio with or without glycine loading test. According to the age of presentation the number of patients in each form of atypical NKH include: the *neonatal* form (eight patients), the *infantile* form (28 patients), and the *late onset* form (11 patients). Three patients are described as asymptomatic. In two of them treatment was initiated soon after birth. The mean CSF/plasma glycine ratios, the mean CSF glycine and the prevalence of different clinical symptoms in the three different forms are shown in Table 2.

Clinical characteristics

In the *neonatal* form of atypical NKH the presentation can be similar to classical NKH with hypotonia and apneic episodes that may require assisted ventilation, though seizures are less severe. Subsequently psychomotor development is significantly better than in the majority of patients with the classical NKH and, in exceptional cases, normal development is reported that may (cases 20a, b, c) [11] or may not (case 31b) [12] be associated with early therapeutic intervention.

The *infantile* form is the most common presentation of atypical NKH. Infants present with a mild to moderate psychomotor delay, after nearly normal development for the first 6 months of life. Seizures, occurring in less than half of them, can be of any type (infantile spasms, partial complex or generalized tonic or tonic-clonic seizures) and are fairly easy to control with anti-epileptics. Occasionally, intermittent or persistent ataxia and choreoathetosis may complicate the presentation. Gross motor development can range from normal to moderately delayed (walking achievement by age 18 months to 6 years), but coordination may be poor. Development progresses and during childhood a mild to moderate developmental delay affecting mostly expressive language is apparent. Behavioral problems are common and occasionally difficult to control. Tem-

Table 1

Clinical and biochemical data of published cases with atypical NKH

Siblings	Type/Gender <i>Neonatal: <1m</i> <i>Infantile: 2m-2y</i> <i>Late onset: >2y</i>	Symptomatology	Ratio		GCS activity Lymphoblasts (pmol/mg) Liver (nmol/mg) or Other testing	Genotype	Ancillary testing	Treatment	Reference
			CSF / plasma glycine	CSF glycine					
Confirmed diagnosis of NKH based on genetic or enzymatic testing									
1	a Infantile/♀	-Infantile spasms (6m) -Mild MR (14y)	0.020	7.4 μmol/L	Lymph: normal Liver: 0.5 ↓ (2.1-3.8)		EEG(6m): Hyps MRI: normal	SB: ↓glycine levels, ↓sz	[20]
2	b Late onset/♂	-Mild dd mostly expressive language (9y)	0.020	7.4 μmol/L			EEG: normal		
3	Infantile/♂	-Mild dd (7m) -Encephalitis-like episodes (2y) -Mild MR (11y)	0.060	51 μmol/L	Lymph: 0.8↓ (4.4-29) Liver: 0.4↓ (2.1-4.6)		EEG: Epil, IPDA (7m) MRI: ↑ T2 signal in thalamus b/!		[38]
4	Infantile/♀	-Hypotonia, infantile spasms (6m) -Mild global dd -Behavioral (irritability aggression)	0.07-0.08	66 μmol/L	Liver: 9.7↑ nkat/kg protein (>112)		EEG(6m): Hyps EEG(22m): Epil CT (6m): normal MRI (21m): normal	SB: improvement DMF: no change	[39]
5	Infantile/♀	-Episodes of lethargy (12m) -Temper tantrums -Global dd (expressive language) (10y)	0.041	41 μmol/L	Lymph: 0.22↓(0.61-1.6) P-protein component: 0.19 ↓ (0.87-1.5)		EEG(1m,13y): normal CT: normal (13y)	No treatment	[40]
6	a Infantile/♂	-Global dd -Intractable ADHD, aggressiveness (9y) -Profound MR, behavioral problems (22y)	0.070	68 μmol/L	Liver: 0.14 ↓ P-protein: 3.5% of normal		CT (10y): atrophy	Folic acid, SB, pyridoxine: no effect	[24]
7	b Infantile/♀	-Global dd (6m) -Severe MR (15y)	0.097	42 μmol/L	Liver: 1.0↓ (3.9-5.2) T protein: 0.3↓ (52.1-77.9)				[41]
8	Infantile/♂	-Moderate dd (27m)	0.097	72 μmol/L	Liver: 1.4 ↓(3.9-5.2) T protein (sibling)				
9	a Infantile/♂	-Epilepsy (6m) -Global dd (language), microcephaly -Moderate MR, outbursts of rage (36y)	-	31 μmol/L	Lymph: 36↓(700nkat/kg) Glycine load: seizure, B-S pattern on EEG			Low-glycine diet: no effect	[28]
10	b Infantile/♀	-Myoclonic seizures (6wks) -Apneic spells	0.060	31 μmol/L	Liver: 0.7 ↓ (3.8-9.5)				[42]
11	a Infantile/♀	-Myoclonic jerks hypotonia (6m) -Severe global dd (5y)	0.090	42 μmol/L	Liver: 1.0↓ (3.8-9.5) T-protein: 0.3↓(30.2-77.9)			SB: no effect	[2,14]
12	b Infantile/♀	-Treatment with strychnine+ arginine started at 9d and SB was added at 15d -Normal development (1y) -Mild dd (27m), Mild MR (9y)	0.100	72 μmol/L	Liver: 1.4↓ (3.8-9.5)	AMT gene: G47R(exon 2) / R320H(exon 8)		SB, strychnine, arginine: ↑CSF glycine, better cognitive outcome	
13	Infantile/♂	-Hypotonia, global dd (language) -Ataxia, choreoathetoid movements -Mild MR (he can keep a job) (21y)	0.050	55 μmol/L		GLDC gene (exon 9): c.1166C>T A389V homozygous Expression analysis A389V: 8%			[32]
14	Infantile/♂	-Hypotonia, seizures (2m), global dd -Epilepsy, choreoathetoid movements -Severe MR, behavioral problems (25y)	0.090	150 μmol/L		GLDC gene (exon 9): c.1166C>T A389V homozygous Expression analysis* A389V: 8% *relative activity	EEG: slow MRI(21y): atrophy HMRS(21y): no glycine peak		
15	b Infantile/♂	-Hypotonia global dd (language) -ADHD, aggressive behavior (sexual impulsivity) (15y) -Mild MR, (20y)	0.056	36 μmol/L		GLDC gene (exon 9): c.2216A>C R739H homozygous Expression analysis* R739H: 6%	EEG(12y): IPDA MRI(12y): normal HMRS: no glycine peak	SB: no effect DMF: no effect	
16	c Neonatal/♀	-Hypotonia, apnea, global delay -DQ (age 32mo): 28 -Severe MR	0.310	270 μmol/L	Lymphoblast: 0 activity	GLDC gene: R790W(exon 20) / N150T(exon 3) Expression analysis* R790W: 14% N150T: 1%	EEG(neonate): b-s MRI: normal	SB: since age 16 d DMF: since age 16 d Imipr: since age 7y	[23]
17	d Neonatal/♀	-Hypotonia, apnea, seizures -DQ (age 53mo): 58 -Mild MR	0.090	160 μmol/L	Lymphoblast: 0 activity	GLDC gene: L82W(exon 1) / 1821-1831del(exon 15) Expression analysis* L82W: 11%	EEG: Epil MRI: normal	SB: since age 7 d Trp: since age 4 y	
18	e Neonatal (f,g,h) / ♀(2pt) ♂(1pt)	-Neonatal hypotonia, apnea (3pt) -Global dd -Choreoathetoid movements -Epilepsy: GTC seizures (5pt) infantile spasms (2pt) -Behavioral problems -Moderate MR	Ratio (Infantile) a 0.061 b 0.087 c 0.067 d 0.081 e 0.061	CSF glycine (Infantile) a 38 μmol/L b 33 " c 43 " d 54 " e 56 "		GLDC gene (exon 22): c.2216A>C transversion that affects the 3 rd base in codon 869 (proline) homozygous	EEG: Epil (5pt) Hyps (2pt)		[33]
			Ratio (Neonatal) f - g 0.058 h 0.058						
19	Neonatal/♀	-Hypotonia, apnea, feeding difficulties -Expressive language delay -Mild MR	0.099	124 μmol/L		GLDC gene (exon 22): c.2216A>C transversion that affects the 3 rd base in codon 869 (proline) homozygous	EEG: normal HCT: atrophy	SB (2mo) Ketamine (2mo)	

(continued on next page)

Table 1 (continued)

20	a	Neonatal / ♀ -Hypotonia, apnea (mechanical ventilation) -Normal cognition (10y)	0.103 124 µmol/L		GLDC gene (exon 20): c.2405C>T A802V homozygous Expression analysis* A802V: 32%	BEG: normal MRI: normal 1HMRS no glycine peak BEG: normal	SM (1d)	[11]
	b	Asymptomatic/♀ -Normal development -Normal cognition (6y)	0.056 127 µmol/L				SB (8d) Ketamine (8d)	
	c	Asymptomatic/♀ -Normal development (10m)	0.077 78 µmol/L				SB (2d) Ketamine (2d)	
21	Neonatal/♀	-Hypotonia, apnea -Normal development (11m) -Neurological deterioration (14m)	0.074 93 µmol/L		GLDC (gene exon 20): c.2405C>T A802V homozygous Expression analysis* A802V: 32%			
Diagnosis of NKH based on increased CSF/Plasma glycine ratio								
22	Late onset/♀	- Visual acuity (13y), seizure, - Normal cognition, optic atrophy (33y)	0.032 27 µmol/L			BEG(33y): Epil MRI: normal (33y)	B6, folic acid: no improvement	[43]
23	Late onset/♀	-dd (11y) -episodes of encephalopathy (31y and 42y) -Ataxia, choreoathetoid movements -Behavioral problems -Mild MR (41y)	0.071 68 µmol/L			BEG: IPDA HCT: cerebellar calcifications	DMF (42): improvement SB (42): improvement	[44]
24	a	Late onset/♀ -Mild global dd (language) (4y) -Intractable ADHD	0.060 36 µmol/L				SB: +glycine / no improvement Trp: no effect Imipr: improvement	[45]
	b	Infantile/♂ -Normal development -Behavioral problems	0.045 30 µmol/L				No treatment	
25	a	Infantile/♂ -Encephalitis-like episode (22m) with -Choreoathetoid movements -Mild global dd (expressive language) -9y WISC-R: IQ: 76	0.120 42 µmol/L	Oral glycine tolerance test: failure glycine to convert to serine		BEG(preload): normal BEG(afterload): Slow	Dietary modification (5 weeks): +glycine, improvement of behavior	[27]
	b	Infantile/♀ -Encephalitis like episode (lethargy irritability, dysmetria) (8m) -Choreoathetoid movements (3y) -Mild MR (expressive language) (7y)	0.160 52 µmol/L	Oral glycine tolerance test: failure glycine to convert to serine		BEG: normal (preload) Slow(after load)	Dietary modification (5 weeks): +glycine, improvement of behavior	
26	Late onset/♂	-Optic atrophy at (4y) -Spastic paraparesis (9y) -Spinocerebellar degeneration (15y)	0.060	Oral glycine tolerance test: failure glycine to convert to serine		CT: atrophy (pons, cerebellar)		[46]
27	Late onset/♀	-Mild MR -Progressive cerebellar ataxia at (40y) -Spastic paraparesis, Babinski (66y)	↑			MRI: hypoplasia of CC, mild diffuse atrophy		[16]
28	a	Infantile/♀ -Epilepsy 11m, -Global dd (expressive language) -Behavioral problems (13y) -Choreoathetosis, dementia (34y)	0.088 135 µmol/L			CT: normal	No treatment	[47]
	b	Infantile/♂ -Epilepsy 1y, -Uncontrolled behavior 14y -Moderate MR, slowly progressive (17y)	0.088 93 µmol/L			CT: normal	No treatment	
29	Infantile/♀	-Lethargy, hypotonia, hyperacusis (6m) -Epilepsy (9m) -Died at 15m: (cystic degeneration of WM, gliosis sparing the U fibers)	0.171 78 µmol/L	Oral glycine load: failure to convert to serine		BEG(9m): Epil	Strychnine: no effect	[15]
30	a	Late onset/♂ -Mild dd, expressive speech delay, (12y) -Episodes of ataxia, irritability	0.053 (baseline) 32 µmol/L(baseline)	0.11 (episode) 62µmol/L(episode)		BEG(during episode): slow		[13]
	b	Late onset/♂ -Normal intelligence (10y) -Expressive language, fine motor delay -Hyperactivity	0.042 25 µmol/L					
	c	Late onset/♂ -Normal intelligence (6y) -Marked expressive language delay -Hyperactivity	0.070 42 µmol/L					
31	a	Infantile/♀ -Mild dd (expressive language), mild hypotonia (29m)	0.100 66 µmol/L			BEG(11m, 20m, 29m): normal	Low protein formula: no effect	[19]
	b	Asymptomatic/♂ -Normal at 15m	0.246 163 µmol/L			BEG(8m, 15m): normal		
32	a	Late onset/♂ -Spasticity and leg weakness (10y) -Normal cognition, spastic diplegia, peroneal muscle atrophy, pes cavus (19y)	0.035 160µg/100ml	Oral glycine load: failure glycine to convert to serine		BMG: Neuropathic changes		[17]
	b	Late onset/♂ -Spasticity and leg weakness -Normal cognition, spastic diplegia, peroneal muscle atrophy, pes cavus (23y)	0.025 180µg/100ml	Oral glycine load: failure glycine to convert to serine				
	c	Late onset/♂ -Abnormal gait (2y) -Spasticity and contractures (8y) -Normal cognition, spastic diplegia, peroneal muscle atrophy, pes cavus (10y)	-	Oral glycine load: failure glycine to convert to serine				

dd: developmental delay, MR: mental retardation, Hysp: Hypsarrhythmia, IPDA: Intermittent Polymorphic Delta Activity, Epil: Epileptiform discharges, ¹HMRS: proton MR spectroscopy, CC: corpus callosum, SB: Sodium Benzoate, DMF: Dextromethorphan, Trp: Tryptophan, Imipr: Imipramine, m: month, y: year, sz: seizures.

* Expression analysis of glycine decarboxylase in COS7 cells and measurement of the relatively activity of glycine decarboxylase.

Table 2

Comparison of clinical and biochemical features of neonatal, infantile, and late onset atypical NKH cases^a

Biochemical marker	Neonatal (n = 8)	Infantile (n = 27)	Late onset (n = 9)
CSF/plasma glycine ratio ^b (≤ 0.02) ^c	Mean: 0.11 Range: 0.06–0.25	Mean: 0.08 Range: 0.02–0.17	Mean: 0.05 Range: 0.03–0.07
CSF glycine ^b (3.8–8.0 $\mu\text{mol/L}$) ^c	Mean: 126 Range: 56–270	Mean: 56 Range: 7–150	Mean: 38 Range: 25–68
Symptomatology	Neonatal (n = 8)	Infantile (n = 28)	Late onset (n = 11)
Epilepsy	3(43%)	12 (39%)	1 (9%)
Hypotonia	8(100%)	18(69%)	—
Episodic presentation	—	4(14%)	2(18%)
Choreoathetosis	3(37%)	11(43%)	2(18%)
Optic atrophy	—	—	2(18%)
Spinocerebellar syndrome	—	—	6(54%)
Peripheral neuropathy	—	—	3(27%)
Behavioral problems	4(50%)	16(57%)	5(50%)
Cognitive impairment ^d			
None	1(12%)	2(7%)	5(45%)
Mild	3(37%)	9(32%)	6(55%)
Moderate-severe	4(50%)	17(61%)	—

^a The reported asymptomatic cases are not included.^b Initial values as reported on the reference before any medical treatment.^c Normal control values may differ between laboratories.^d According to the clinical description or to a formal IQ testing.

per tantrums and irritability dominate the picture initially, followed by outbursts of aggressiveness and rage later on. Attention deficit hyperactive disorder (ADHD) resistant to treatment with psychostimulants and mild expressive language delay may be the only symptoms in some cases. An episodic presentation induced by a febrile illness has been described in some patients with lethargy, flaccidity, ataxia, choreoathetoid movements, gaze palsy, paroxysmal screaming, and delirium. A patient with an episodic presentation (case 30a) was studied during the episode and was found to have higher CSF glycine levels and CSF/plasma glycine ratio than during the baseline [13]. The reason for the intermittent glycine increase is unknown but may be related to the metabolic stress during an illness that can further compromise the deficient mitochondrial GCS activity. Overall the phenotype is consistent with a static encephalopathy and, although the outcome is better than the classical one, 61% of cases will have a moderate to severe cognitive impairment. In addition, neurological deterioration has been described in some cases (cases 9b, 21, 29) [11,14,15] despite the mild initial symptomatology.

The *late onset* form is less common and more heterogeneous. The clinical presentation is after the second birthday and even during adulthood, mainly with mild cognitive decline and behavioral problems. In a few cases, a slowly progressive spinocerebellar syndrome including ataxia, upper-motor neuron signs, optic atrophy, and peripheral neuropathy has been described. Persons with late onset NKH tend to have a normal life span and the oldest reported case is 66 years old [16]. A sibship of three males has been described with a pecu-

liar phenotype of progressive lower extremity spasticity, leg weakness, peroneal muscle wasting, and neuropathic changes on EMG; the diagnosis of NKH was based on mild elevation of CSF/plasma glycine ratio and on abnormal glycine tolerance test [17]. Although a deficient GCS is speculated, the cause of the hyperglycemia in these *late onset* cases is unknown, since they all lack enzymatic or genetic confirmation.

In classical NKH, on a retrospective natural history study [18], females were found to have a more severe disease. However, no such gender predilection was found in published cases of atypical NKH. Siblings are expected to be concordant in clinical and biochemical phenotypes. However, discordance for age at presentation, clinical severity, and glycine levels, which may [14] or may not [19,20] be related to treatment, has been reported.

Metabolic characteristics and pathogenesis

A CSF/plasma ratio higher than 0.08 is considered diagnostic of classical NKH [8] but atypical NKH cases can have lower ratios. The mean CSF/plasma glycine ratios, in *neonatal* form of atypical NKH of 0.11 (range 0.06–0.25) and in *infantile* form of 0.08 (range 0.02–0.17), differ substantially from the mean ratio of 0.23 (range 0.07–0.70) described by Applegarth and Toone[8], in 25 classical NKH cases with enzymatic confirmation. However, there is much overlap and, when the clinical presentation is during neonatal period, the CSF/plasma glycine ratio alone is not a reliable test to identify those rare patients with a potentially favorable

outcome. Moreover, the few reports on transient NKH with severe disease in the newborn period and subsequent clinical and biochemical resolution [21] complicate even more the decision-making about aggressive supportive management and early therapy. In *late onset* form of atypical NKH the mean CSF/plasma glycine ratio is even lower at 0.04 (range 0.03–0.07) and none had a ratio above 0.08, that is considered a diagnostic threshold for the classical form.

There is debate whether the CSF/plasma glycine ratio is correlated with the prognosis in classical NKH. For atypical NKH, all cases described with “normal cognition” had a ratio less than 0.10 except for one extreme outlier (case 31b) with a ratio of 0.25 and “normal development” at the age of 15 months [19]. The lowest ratio level described in an atypical NKH with moderate or severe mental retardation is 0.06. Hence, we consider a ratio lower than 0.06 a promising factor for a better outcome. The stratification of atypical cases by cognitive outcome shows that there is a trend for cognitive impairment to be associated with higher CSF/plasma glycine ratio (Fig. 1). *Late onset* atypical NKH have lower ratios and better cognitive outcome. The above picture, extrapolated by the literature review, is a gross estimate since a validated measurement of the cognitive outcome and the timing of therapeutic intervention are often lacking.

The metabolic defect in *neonatal* and *infantile* forms of mild NKH is usually an abnormality in the P-protein or less commonly in the T-protein of GCS, whereas the metabolic defect in *late onset* form is unknown. In the classical NKH, the overall GCS activity is usually very

low or undetectable in liver tissue and brain [22]. Generally in atypical forms a higher hepatic and lymphoblast GCS activity is observed. However, there are reported cases with low hepatic (case 1a) [20] or lymphoblast (cases 13, 14) [23] GCS activity, in the classical NKH range, and mild clinical phenotype. This discrepancy exists presumably because liver and lymphoblast GCS activity does not absolutely reflect brain GCS activity [24].

Glycine accumulation in the CNS has been assumed to exert its toxic effect primary through *N*-methyl-D-aspartate (NMDA)-mediated excitotoxicity in the cerebral cortex, hippocampus, and cerebellum as well as through enhanced direct inhibition in the spinal cord and brain stem [25]. Much research supports the toxic effect of glycine on neuronal activity. Intraventricularly administered glycine potentiates seizures in animals [26] and an oral glycine load can cause lethargy, precipitate seizures, and induce slow activity and even burst-suppression EEG patterns in patients with *infantile* NKH [27,28]. Common manifestations of atypical NKH patients are the mental retardation and behavioral problems. Since the NMDA receptor complex is involved in many functional processes including neural development, synaptic plasticity and learning and memory [29], a cognitive dysfunction is not surprising with NMDA dysregulation caused by the abundant CNS glycine. Studies in animals showed a causative role of glycine binding site of the NMDA receptor in inducing defensive behavior and anxiogenic-like reaction, which may be reversed by non-selective glycine B receptor antagonists [30]. Two observations support the idea that the neuropathogenesis may arise in part from the deficient GCS activity per se and not merely from the toxic effect of glycine. First, there are a few cases with low hepatic CGS activity and neurological impairment despite normal CSF glycine [20] and second, successful lowering of the CSF glycine concentration with therapy, does not always improve neurological function. The GCS is abundantly expressed in neural stem cells in developing brain, and generates one-carbon unit (5,10-methylenetetrahydrofolate) that is required for DNA synthesis [31]. Deficiency of the GCS activity may cause irreversible damage to embryonic brain, resulting in poor long-term neurological outcome.

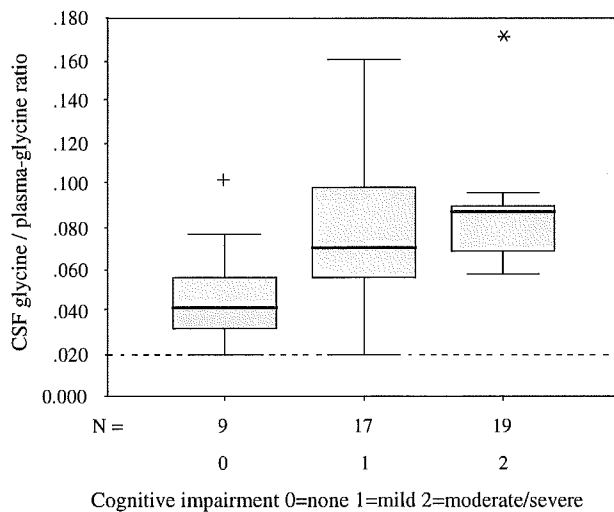


Fig. 1. CSF/plasma glycine ratio and cognitive outcome. Published atypical NKH cases were stratified grossly by measures of cognitive function (see text), and CSF/plasma glycine ratios were compared, excluding case 31b, an extreme outlier whose cognitive function could not be assessed reliably at 15 months (apparently normal). A trend of cognitive impairment to associated with higher CSF/plasma glycine ratios was observed ($p = 0.07$). Notice the overlap of the CSF/plasma glycine ratios between groups. †(case 20a), *(case 29).

Molecular studies

The first genetic characterization in atypical NKH was in a patient with T-protein defect harboring two different missense mutations G47R and R320H in the *AMT* gene [2]. To date three missense mutations (A389V, R739H, and A802V) on the *GLDC* gene have been identified in homozygous state in *neonatal* and